June 2004

The Effects of Porphyromonas Gingivalis Lipids on Atherosclerosis Formation in Mice.

Steven Robert Sierakowski

The Effects of *Porphyromonas gingivalis* Lipids on Atherosclerosis Formation in Mice

Steven Robert Sierakowski

B.S., Villanova University, 1998

D.M.D., University of Pennsylvania, 2001

A Thesis

Submitted in Partial Fulfillment of the

Requirements for the Degree of

Master of Dental Science

at the

University of Connecticut

2004

APPROVAL PAGE

Master of Dental Science Thesis

The Effects of *Porphyromonas gingivalis* Lipids on Atherosclerosis Formation in Mice

Presented by

Steven Robert Sierakowski, B.S., D.M.D.

Major Advisor_____
Frank C. Nichols

Associate Advisor_____
Arthur R. Hand

Associate Advisor_____
John W. Dean, III

University of Connecticut

2004

To the memory of my mother, Nina, whose love will never be forgotten,

And

To my father, Robert, whose own academic leadership has inspired me to further my education, and whose unwavering love and support encouraged me to persevere.

Acknowledgments

I would like to thank my major advisor, Dr. Frank Nichols, whose dedication to academic excellence created an environment conducive to learning and personal merit; and my associate advisors, Dr. Arthur Hand and Dr. John Dean, whose generous time and thoughtful suggestions are deeply appreciated.

I would also like to acknowledge Dr. Robert Clark for graciously providing practice specimens; Mr. David Serwanski for valuable assistance with histological techniques; Ms. Susan Krueger for kind help with the computer-assisted analysis; and the faculty of the Department of Periodontology for their encouragement.

TABLE OF CONTENTS

Introduction.....1

Objective.....19

Materials and Methods.....20

Results.....31

Discussion.....35

Conclusion.....44

Figures.....46

References.....54

LIST OF FIGURES

Figure 1: Table illustrating the number of mice per group that died after a single intraperitoneal injection of each solution.....46

Figure 2: Histogram comparing the final mouse body weights per treatment group fed either normal or high-fat chow.....47

Figure 3: Representative aortic cross-sections (4x) from a mouse injected with 2.5 µg of the total lipid extract stained with Oil red O and counterstained with Mayer's hematoxylin.....48

Figure 4: Higher magnifications of an aortic cross-section from a mouse injected with 2.5 µg of the total lipid extract illustrating the steps used for analysis.....49

Figure 5: Histogram comparing the percent lipid deposits (defined by pixel counts) within the proximal aortic wall per treatment group fed either normal or high-fat chow.....50

Figure 6: Histogram comparing the relative abundance of 3-OH *iso*$C_{17:0}$ recovered from descending aortas per treatment group fed either normal or high-fat chow.....51

Figure 7: Chemical structure of *Porphyromonas gingivalis* HPLC lipid fraction 17 ceramides.....52

Figure 8: Chemical structure of *Porphyromonas gingivalis* HPLC lipid fraction 28 ceramides.....53

INTRODUCTION

Periodontal disease is one of the most common pathogenic conditions to affect the human oral cavity [1]. Its most common form, chronic periodontitis, is caused by a bacterial-induced chronic inflammatory reaction, which ultimately destroys the attachment apparatus of the dentition [2]. As a supragingival biofilm, largely composed of Gram-positive aerobic microorganisms, accumulates apically along the tooth surface, a new ecological niche is created enabling the predominately Gram-negative anaerobic flora commonly found in periodontal pockets to thrive [3]. Specific bacteria cultured from periodontal pockets have been described as more pathogenic than others, namely *Actinobacillus actinomycetemcomitans*, *Prevotella intermedia*, *Tannerella forsythensis*, *Porphyromonas gingivalis*, and *Treponema denticola* [4, 5], and have been shown to adversely affect the outcome of periodontal therapy [6]. In fact, *P. gingivalis*, known to be one of the most pathogenic microorganisms recovered in the gingival crevice, can be isolated in high numbers and prevalence in patients with chronic and aggressive forms of periodontitis. By contrast, periodontally healthy patients will have either no *P. gingivalis* or only small quantities in subgingival plaque. A shift in bacterial flora to include these organisms is associated with an increase in the inflammatory cell infiltrate within the gingival epithelium and connective tissue, leading to a release of inflammatory mediators including interleukin-1β (IL-1β), interleukin-6 (IL-6), interleukin-8 (IL-8), tumor necrosis factor-α (TNF-α), prostaglandin E_2 (PGE_2), and matrix metalloproteinases (MMPs), which recruit lymphocytes, fibroblasts, and osteoclasts that degrade the surrounding periodontal tissues.

The subgingival microflora at destructive inflammatory disease sites elicits the complex host immune response through virulence factors such as endotoxin, lipoproteins, proteases, and lipopolysaccharide (LPS). Of these, the most studied by far has been LPS, which is a cell wall constituent of Gram-negative microorganisms. Although evidence for the penetration of LPS into gingival tissue has been reported [7, 8], its location in these tissues at human disease sites is questionable. It has been demonstrated, however, that entire bacteria, including *P. gingivalis*, can penetrate the connective tissue through micro-ulcerations within pocket epithelium, thus contaminating these tissues with LPS [9, 10]. This, though, does not appear to be the main mode for the destruction of the periodontium since the invasive bacterial counts are minimal [11]. Instead, many periodontal pathogenic microorganisms bind to pocket epithelial cells, exposing these and neighboring host inflammatory cells to LPS and other virulence factors. Bacterial lipopolysaccharide acts by binding to the LPS-binding protein (LBP), a plasma protein [12]. The LPS-LBP complex then binds to both soluble and membrane-bound CD-14 on peripheral blood monocytes, macrophages, or vascular endothelial cells, resulting in intracellular signaling to upregulate cytokine gene transcription. In fact, Schumann and coworkers reported that the LPS-LBP complex is 1,000-fold more active than LPS itself in stimulating TNF-α synthesis from macrophages [13]. However, a later study indicated that blocking the CD-14 receptor with antibodies had no effect on the TNF-α production if the LPS concentrations were sufficiently high, indicating that other receptors may be involved [14].

Recently, researchers have identified a family of evolutionarily conserved microbial pattern-recognition receptors known as Toll-like receptors (TLRs). Receptors

in this family have an intracellular domain which shares homology with the IL-1 receptor. Activation of TLRs initiates a signal transduction cascade leading to the activation of nuclear factor-kappa B (NF-κB) and eventual production of the pro-inflammatory cytokines TNF-α, IL-1, IL-6, and IL-8 [15]. It appears that most Gram-negative LPS binds to TLR-4 [16, 17], although conflicting data have demonstrated that *P. gingivalis* LPS may also bind to TLR-2 [18, 19]. Thus, LPS can either directly or indirectly induce the secretion of pro-inflammatory mediators from surrounding peripheral blood monocytes, macrophages, and other host cells. These mediators then amplify the inflammatory cytokine cascade leading to the destruction of the periodontal attachment apparatus.

Of all the known periodontal pathogens, *Porphyromonas gingivalis*, an obligately-anaerobic Gram-negative asaccharolytic coccobacillus, seems to be one of the most virulent. Its prominence is related to the expression of many phenotypic factors including fimbrial adhesins, LPS, collagenase, and trypsin-like enzymes. Recently, researchers have discovered two fimbrillin proteins, one 41-kDa and the other 67-kDa, on the *P. gingivalis* cell surface which were shown to aid in the adherence to gingival epithelial cells [20]. Furthermore, *P. gingivalis* produces cysteine endopepdidases known as gingipains which account for 85% of the general proteolytic activity and 100% of the trypsin-like activity of this periodontal pathogen [21]. Gingipain K releases bradykinin from high molecular weight kininogen, and has strong fibrinolytic activity which may contribute to clinical bleeding on probing in patients with periodontitis. Gingipain R activates thrombin production, which has pro-inflammatory actions, and degrades C3, a complement protein whose cleavage results in opsonization and neutrophil chemotaxis.

Furthermore, both gingipains inactivate IL-8, another potent neutrophil chemoattractant. More importantly, these enzymes degrade macrophage CD-14, thereby inhibiting the activation of leukocytes through the LPS receptor. Such a finding is corroborated by the fact that *P. gingivalis* LPS is not as potent a stimulator of PGE_2 secretion from human monocytes *in vitro* when compared with other suspected periodontal pathogens [22]. All of these factors can modulate bacterial capacities for cellular attachment, invasion, or destruction.

The lipopolysaccharide molecule contains three structural components: an O-specific polysaccharide, a core polysaccharide, and Lipid A. It has been demonstrated that the Lipid A portion of the molecule is responsible for inflammatory cell activation, and its potency differs among bacterial species [23]. Covalently bonded to Lipid A by either amide or ester linkages are even carbon-chain 2-hydroxy and odd-chain isobranched 3-hydroxy fatty acids. Interestingly, these fatty acids are also found linked to long-chain bases, forming complex lipids of the sphingolipid class called ceramides [24]. Periodontal pathogenic microorganisms of the *Bacteroides*, *Porphyromonas*, and *Prevotella* genera synthesize several hydroxy fatty acids, one of which is 3-hydroxy-15-methylhexadecanoate (3-OH *iso*$C_{17:0}$) [25]. The predominant hydroxy fatty acid of most Gram-negative bacteria is 3-OH $C_{14:0}$, but more than 50% of the fatty acid of *P. gingivalis* is 3-OH *iso*$C_{17:0}$ [26]. Furthermore, even though mammalian cells have not been shown to produce 3-OH *iso*$C_{17:0}$, this fatty acid has been recovered in lipid extracts of periodontally diseased human cementum and gingival tissues [27]. Additionally, it is now established that most of the sphingolipid recovered from *P. gingivalis* are free and phosphorylated dihydroceramides, which include 3-OH *iso*$C_{17:0}$ in amide linkage to long-

chain bases of 17, 18, and 19 carbons in length [28]. These specific ceramide lipids of *P. gingivalis* are biologically active, promoting a markedly greater secretion of PGE_2 from IL-1β-treated gingival fibroblasts than is observed with IL-1β alone [29].

Since these bacterial ceramides, some of which contain 3-OH *iso*$C_{17:0}$, but not LPS, are virtually insoluble in aqueous solution, a novel mechanism of bacterial lipid deposition and systemic infiltration has been proposed by Nichols [27]. Although the bacterial hydroxy fatty acids may be separated from the Lipid A portion of LPS and retained in the gingival tissues, these fatty acids would not be expected to link to saturated long-chain bases as is observed in ceramides of *P. gingivalis*. Stated another way, recovery of bacterial ceramides in diseased human tissue samples is not likely to represent breakdown of *P. gingivalis* LPS and subsequent incorporation of bacterial fatty acid into host sphingolipids. Additionally, because 3-OH *iso*$C_{17:0}$ is not recovered in plasma from patients with periodontitis, it is unlikely that *P. gingivalis* lipids are taken up and carried freely in this medium. Instead, since 3-OH *iso*$C_{17:0}$ is recovered in circulating blood cells in patients with periodontitis, it is possible that *P. gingivalis* lipids are incorporated into cell membranes of circulating blood cells, particularly phagocytes. In fact, there is evidence suggesting that *P. gingivalis* sheds outer membrane vesicles in culture medium during growth [30]. Other research has shown that human gingival fibroblasts [29] and peripheral blood monocytes (Nichols, unpublished data) take up such complex lipids of *P. gingivalis* as evidenced by the facile incorporation of these lipids when cells are plated on culture surfaces coated with bacterial lipid. Assuming the same is true in blood, the frequent bacteremias associated with periodontal disease [31, 32] would be expected to contaminate circulating blood cells with these biologically active

lipids. Furthermore, the attachment of *P. gingivalis* to junctional and sulcular epithelial cells [33] or its invasion into periodontal connective tissue [34] could also provide a source of bacterial lipid to surrounding host inflammatory cells. Thus, monocytes and macrophages at the infected periodontium could incorporate the lipids into their own cell membranes and deliver them to other tissues, including arterial walls susceptible to atherosclerosis.

Atherosclerosis pathogenesis

Atherosclerosis is the most common form of arteriosclerosis, which refers to the thickening of vessel walls [35]. It is a pathologic process which has become the leading cause of human vascular disorders including coronary artery disease (CAD), cerebrovascular disease, and diseases of the aorta and peripheral arterial circulation. These vascular diseases are responsible for more deaths than any other disease in humans. The hallmark of the atherosclerotic lesion is the accumulation of lipid within the vessel wall and subsequent fibrosis and calcification of the connective tissue, which eventually obstructs blood flow through the lumen, predisposes the vessel to thrombosis, and weakens its elasticity in response to hydrodynamic stresses. Although there have been numerous risk factors attributed to the cause of atherosclerosis such as hypertension, diabetes mellitus, cigarette smoking, increased age, physical inactivity, hyperhomocystinemia, hypercoagulability, and angiotensin-converting enzyme polymorphisms, hyperlipidemia seems to be the most studied factor. However, like

periodontal disease, atherosclerosis is considered to be a chronic inflammatory disease, sharing similar inflammatory and immunological mediators [36].

Histologically, blood vessel walls are composed of three distinct layers: the tunica intima, tunica media, and tunica adventitia [37]. The innermost layer, the tunica intima, contains a single layer of squamous epithelial cells, called endothelium, which rests on a basal lamina. The subendothelial connective tissue may contain smooth muscle cells, sporadic macrophages and lymphocytes, and, in arteries, a layer of fenestrated elastic tissue known as the internal elastic lamina. The tunica media is largely composed of circumferentially arranged smooth muscle cells with interposed elastin, reticular fibers, and proteoglycans. It extends from the internal elastic lamina to the external elastic lamina, which is a thin layer of elastin separating the tunica media from the tunica adventitia. This third layer is composed mostly of collagen, microvasculature, lymphatics, and loose connective tissue surrounding the vessel.

Arteries are distinguished from one another by the thickness and composition of the various layers; and are categorized by size into large (elastic) arteries, medium (muscular) arteries, small arteries, and arterioles. The large arteries such as the aorta and pulmonary arteries are extremely elastic to accommodate the high blood pressure generated by contraction of the ventricles. Thus, the tunica media is the thickest layer in these arteries consisting of concentric layers of elastin and sheets of smooth muscle cells. The intima is also relatively thick with an inconspicuous internal elastic lamina. Medium sized arteries have much more smooth muscle and less elastin in the tunica media than large arteries. These arteries are thus more apt to contract, aiding in the regulation of blood pressure. Furthermore, they have a more distinct internal elastic lamina and a

thicker tunica adventitia. By contrast, small arteries and arterioles have only 1-8 layers of smooth muscle cells in their tunica media, a thin tunica intima, and a tunica adventitia which blends into the surrounding connective tissue.

Atherosclerosis occurs mainly in large and medium sized arteries. In humans, the most commonly affected vessels are the abdominal aorta, coronary arteries, aortic arch, descending thoracic aorta, internal carotids, femoral and iliac arteries, and the Circle of Willis. However, the location of occurrence varies in other animal species. Evidence suggests that the majority of lesions are associated with branch points or areas of low shear stress [38]. Although controversial, the earliest sign of atherosclerosis is intimal thickening, in which a layer of connective tissue separates the endothelium from the internal elastic lamina. Some argue that this finding may be an adaptive response to normal vessel stress, but most agree that these sites are most likely to develop atherosclerosis. It is at these lesion-prone sites that lipid will most commonly accumulate in arterial walls.

The American Heart Association has recently defined six stages of atherosclerotic lesion development [39, 40]. The type I lesion is defined as the first microscopically and chemically detectable lipid deposits not visible to the naked eye. The type II lesion is known as the fatty streak, which is a small yellow lump in the vessel wall consisting of lipid-laden macrophages and smooth muscle cells known as foam cells. Much of the lipid at this stage is intracellular. The type III lesion represents a transitional stage between fatty streaks and advanced lesions. The hallmark of this stage is multiple extracellular lipid pools which do not have a clearly delineated acellular lipid core. Type IV lesions have this well-defined acellular lipid core usually at the deepest portion of the tunica

intima. This core is largely composed of cholesterol esters and cholesterol, as well as necrotic foam cells. Calcifications mostly composed of apatite crystals are also found at the musculoelastic junction. Once smooth muscle cells are found surrounding the core flanked by groups of macrophages and lymphocytes (known as a fibrous cap), the type V lesion is established. Finally, the type VI lesion is marked by loss of surface integrity, ulceration, hematoma formation, and eventual thrombus formation.

The atherogenic process is initiated by a mechanical or biochemical injury to the arterial endothelium, enabling increased adherence of peripheral blood monocytes and platelets, and enhanced permeability of monocytes, macrophages, and lipoproteins into the intima. Both ingested and endogenously synthesized cholesterol is transported to and from the liver by lipoproteins in the plasma and lymph. One specific lipoprotein, low-density lipoprotein (LDL), carries most cholesterol in the form of cholesterol esters. LDL and other lipoproteins, such as very low-density lipoprotein (VLDL), accumulate as a result of either high-lipid dietary intake or increased hepatic cholesterol synthesis. Free-radical oxidative metabolites of endothelial cells and monocytes then initiate lipid oxidation within the lipoproteins. The resulting oxidized LDL (oxLDL) has been shown to up-regulate adhesive proteins such as vascular cell adhesion molecule-1 (VCAM-1), intercellular adhesion molecule-1 (ICAM-1), E-selectin, and monocyte chemotactic protein-1 (MCP-1) [41], which aid in the adhesion, rolling, and diapedesis of leukocytes. It should be emphasized that elevated expression of these adhesion molecules is also promoted by inflammatory cytokines such as IL-1β and TNF-α. In conjunction with these proteins, oxLDL exacerbates the endothelial dysfunction by oxidatively modifying cell membrane phospholipids, allowing greater adherence and influx of inflammatory

cells into the intima. Furthermore, the excessive production of superoxide anions decreases the bioavailability of nitric oxide (NO), which normally protects the endothelium by inducing vasodilation, inhibiting platelet aggregation and smooth muscle cell proliferation, and blocking endothelial-leukocyte interactions. Additionally, oxLDL enables endothelial cells to express macrophage colony stimulating factor (M-CSF), which stimulates the conversion of monocytes to macrophages in the tunica intima [42], initiating fatty streak formation.

There are several checks produced by the host that play key roles in inhibiting the atherogenic process. The first resides in the control of MMP activity. Although MMPs can be inhibited by plasma α_2-macroglobulin, the tissue inhibitors of metalloproteinases (TIMPs) are the major inhibitory proteins in the connective tissue. TIMPs have complex three-dimensional structures defined by six disulfide bridges creating six loops. The first three loops form high-affinity non-covalent complexes with the propeptide portion of active metalloproteinases, inhibiting their activity. However, the exuberant MMP response to inflammatory cytokines ultimately exceeds TIMP activity, contributing to tissue breakdown. As a second check, high-density lipoprotein (HDL) has been shown to inhibit the oxidation of LDL via two enzymes: platelet-activating factor acetylhydrolase and paraoxonase [43]. HDL has also been shown to hamper the cytokine-induced expression of endothelial cell adhesion molecules, thereby reducing the quantity of monocyte immigration [44]. Finally, excess oxLDL in the intima is internalized by monocytes and macrophages by binding to their acetyl LDL- and oxidized LDL-receptors [45] such as the scavenger receptors CD-36 and CD-68, and LOX-1 [46]. Under normal concentrations of serum LDL, the phagocytic cells degrade oxLDL, ridding arteries of

this inflammatory mediator. However, with elevated serum oxLDL, this scavenger system becomes overburdened, and cholesterol esters accumulate both intra- and extra-cellularly. With the net increase of oxLDL in the intima, endothelial damage occurs and the atheroma lesion precipitates.

As macrophages accumulate within the arterial intima, they take up oxLDL in both cytosolic and lysosomal compartments and are transformed into foam cells [47]. In addition, the decrease of endothelially produced NO promotes proliferation of smooth muscle cells (SMCs) from the tunica media to the intima. If the combination of hyperlipidemia, monocyte adhesion, subendothelial migration of SMCs, and foam cell formation persist, type II lesions (fatty streaks) will be apparent. Interestingly, recent evidence suggests that *P. gingivalis* may stimulate foam cell formation by promoting LDL binding to macrophages and LDL aggregation [48, 49]. Next, T lymphocytes are recruited, which release cytokines signaling macrophages to release MMPs and other proteases, which remodel the extracellular matrix. It has been suggested that MMP activity provides more substrate for heparinase (secreted by macrophages), which may play a role in SMC phenotype modulation [50], upregulating scavenger receptors and increasing lipid accumulation. As the progression continues, platelets aggregate at the dysfunctional endothelium and, along with SMCs, secrete growth factors such as platelet-derived growth factor (PDGF), fibroblast growth factor (FGF), and transforming growth factor-α (TGF-α), mediating cell migration, proliferation, extracellular matrix deposition, and further unwanted gene expression [43]. In fact, it has been shown that some of the proteoglycans have an increased capacity to bind LDL. The atherosclerotic lesion at this

stage consists of an aggregation of foam cells and extracellular lipid surrounded by SMCs and fibrous tissue consistent with the type III lesion, a fibrous plaque.

Sometimes, atheromas undergo considerable connective tissue formation with little central lipid accumulation. Usually, however, the lipid-laden macrophage foam cells eventually show signs of cell death or disintegration, creating a necrotic core in the fibrous plaque typical of the type IV lesion. At this stage, much of the intracellular cholesterol has crystallized. As the lesion increases in size and more SMCs migrate to the plaque, the fibrofatty atheroma becomes the type V lesion. As stated earlier, type VI atherosclerosis consists of rupture and ulceration of the endothelium leading to intraplaque hemorrhage and thrombus formation. However, it appears that type IV and V lesions are just as prone to rupture due to the "shoulders" of macrophages and T lymphocytes along the fibrous cap [51]. These areas tend to be the most unstable, especially when there is a paucity of smooth muscle cells and collagen to contain these clusters. The MMPs produced by macrophage-derived foam cells will further aid in the matrix degradation causing plaque rupture. Thus, the vulnerability of the atheroma depends more on the plaque composition (lipid rich/collagen poor) rather than plaque volume (severity of stenosis). The clinical outcome depends on the location, severity, and duration of the ischemia caused by the occlusion. This can range from differing stages of angina to infarction and stroke.

Murine models of atherosclerosis

Since the study of atherosclerotic plaques in humans has many technical and ethical considerations, the use of animal models has become an acceptable substitute. Recent experiments have used mice, rats, rabbits, hamsters, guinea pigs, chickens, swine, dogs, cats, and monkeys. In general, mice are highly resistant to atherosclerosis. In fact, when fed a low-fat, low-cholesterol diet, they typically have cholesterol levels less than 100 mg/dl, mostly contained in HDL, and do not develop atherosclerotic lesions. Furthermore, wild-type mice generally do not develop significant atherosclerosis when fed high-fat diets.

Of particular interest in current cardiovascular research, inbred, transgenic, and gene-targeted mice are used for advantageous reasons. Transgenic mice are those in which specific genes, which are involved in the regulation of lipoprotein metabolism, are overexpressed. For instance, gene-targeted mice such as those homozygous deficient for apolipoprotein E (apoE) will spontaneously develop fatty streaks progressing to fibrous plaques on a normal diet with cholesterol levels ranging from 400-600 mg/dl; and more expansive lesions on a high-cholesterol diet with cholesterol levels at 1500-2000 mg/dl [52]. Apolipoprotein E is a 34kD glycoprotein component of lipoproteins that is synthesized in the liver, brain, and other tissues. It has been shown to interact with apolipoprotein B-48 and chylomicron remnant receptors to aid in the hepatic metabolism of various apoE-containing lipoproteins such as VLDL and chylomicrons. As another example, transgenic mice that express human apolipoprotein B-100, resulting in increased VLDL and LDL plasma concentrations, will have atherosclerosis development largely consisting of macrophage foam cells when fed high-fat diets [53]. Other genetically engineered mice include those deficient for the LDL receptor, which form

fatty streak lesions when fed a high-fat diet progressing to a necrotic core, but without a fibrous cap [54]. Serum cholesterol levels can reach 1500 mg/dl with the majority composed of LDL and IDL in these mice [55]. In these knockout mice, the earliest lesions appear in the vicinity of the aortic valves. Soon after, other sites with high predilection are affected: the small curvature of the arch; the orifices of the brachiocephalic, left subclavian, and common carotid arteries; the branch sites of the mesenteric and renal arteries; and the iliac bifurcation. The lesions formed at these loci then grow toward the lumen and expand laterally. The speed at which these various knockout mice develop plaques, though, is often too rapid for the determination of the effects of a potential confounding factor.

Of the inbred strains, C57BL/6J mice develop fatty streak lesions consisting of several layers of foam cells in the subendothelial space of their aortas when fed diets consisting of 1.25% cholesterol, 0.5% cholic acid, and 15% fat for several months [56, 57]. Such a diet increases their cholesterol levels two to three-fold (200-300 mg/dl), the majority of which is contained in non-HDL fractions [55]. However, the hypercholesterolemia alone is insufficient to induce significant atherogenesis. The addition of cholic acid to the diet enhances inflammation, and allows the accumulation of macrophages in the aortic intima [47]. As with the transgenic mice, the lesions are first formed under the aortic valve leaflets where turbulent flow is prevalent. Paigen and coworkers have shown that these mice will have 4,500-8,000 μm^2 aortic lesions at 14 weeks, most of which occur at the junction of the aorta and the heart [57]. At nine months, the lesions can encompass 8% of the aortic length. Furthermore, it has been

demonstrated that female C57BL/6J mice will produce larger atherosclerotic lesions than males [58].

All of the experimental mice described, however, will develop lesions in the same inflammatory-fibroproliferative manner as humans [59]. Furthermore, the lesions can be easily dissected and studied both histomorphometrically and with electron microscopy [57]. Thus, because inbred C57BL/6J female mice will not form atherosclerosis at a rate and severity as extensive as other genetically engineered mice, possibly masking the effect of experimentally introduced mediators, they make an excellent model for the development of atherosclerosis in this study.

The epidemiological association between periodontitis and atherosclerosis

Because both chronic periodontitis and atherosclerosis possess similar pathogenic processes as described above, many studies have attempted to find a cause-effect relationship between the two conditions. To date, there are only eight longitudinal studies published describing the effect of periodontal disease prevention or treatment on cardiovascular events [60-67]. Six of the eight suggest that the presence of periodontal disease precedes cardiovascular events, while two found no such relationship. All of the studies vary with regard to patient population, classification of periodontal disease, cardiovascular outcome examined, and adjustments for potential confounders. Because of these differences, comparisons among the studies are limited.

Beck and co-workers [63] analyzed data for 1,147 men from the Normative Aging Study and the Dental Longitudinal Study of the Department of Veterans Affairs. Mean

bone loss and periodontal probing pocket depths were recorded per tooth at baseline and follow-up examinations up to 18 years later. Two hundred seven of the originally healthy patients developed CAD, and forty others succumbed to stroke. After adjusting for age and other cardiovascular risk factors, the odds ratios associated with having at least 20% mean alveolar bone loss were 1.5 for CAD and 2.8 for stroke. Another study by Joshipura et al. [62] followed 44,119 healthy male health care professionals at baseline for 6 years. The authors noted 757 new cases of CAD. A positive correlation for tooth loss due to periodontal disease and CAD was determined with a relative risk of 1.67 after adjusting for standard CAD risk factors. It must be noted, however, that periodontal disease in this population was self-reported as a dichotomous variable, which does not allow for quantification of extent of periodontal disease.

The study conducted by Hujoel and colleagues [65] examined data collected from the first National Health and Nutrition Survey (NHANES I: 1971-1975) with its 21-year follow-up findings. They measured the association between periodontitis as determined by the Russell Periodontal Index with death or hospitalization due to CAD. After adjusting for confounding factors, no association was found for gingivitis, and an odds ratio of only 1.14 was calculated for periodontitis. It is interesting to note that the earlier study by DeStefano et al. [60] used the same NHANES I database with 15 years of follow-up using the same periodontal index and found a statistically significant association between the two diseases with a relative risk of 1.72. It has been postulated that the discrepancy between the two studies is because Hujoel and co-workers either overadjusted for confounding factors which may have been associated with periodontal disease, or misclassified the periodontal status of patients at baseline [68].

Thus, there seems to be some evidence, not necessarily of a cause-effect relationship, but of a moderate correlation between periodontal disease and cardiovascular disease. There are several proposed systemic mediators linking the two diseases: direct bacterial infection, pro-inflammatory cytokines, acute-phase plasma proteins such as C-reactive protein (CRP) and serum amyloid A (SAA), and fibrinogen [69]. The monocyte-derived cytokines such as IL-1, IL-6, IL-8, and TNF-α can induce atherosclerosis by enabling hepatic production of fibrinogen and CRP, which activate complement and cause platelet aggregation. These cytokines also have the potential to increase the expression of cellular adhesion molecules at the vascular endothelium, thereby attracting more monocytes to the intima. Thus, periodontal infection, consisting of a reservoir of specific Gram-negative microorganisms, has the potential to stimulate the cytokine storm either at the inflamed periodontal tissues or in the systemic circulation.

Indirect experimental evidence supports the possibility of direct invasion of major arterial walls by specific periodontal pathogens, particularly *P. gingivalis* [70, 71]. PCR detection of genomic markers for periodontal pathogens indicates that only a small percentage of carotid atheromas are contaminated with *P. gingivalis*, although almost half of human carotid atheromas are positive for the major periodontal pathogens. However, histological verification of artery invasion by periodontal pathogens has not been demonstrated in humans *in situ*. Assuming that periodontal disease in adults predisposes individuals to cardiovascular disease, it appears that either the microbial flora gains entry into the systemic circulation and prompts a more rapid progression of atherosclerosis, or the local inflammatory events associated with periodontal disease spill over into the

systemic circulation to the extent that atherosclerosis progression is accelerated. In fact, both events may be involved in the promotion of atherosclerosis in subjects with periodontal disease.

Recent evidence by Varlamos [72] and Nichols (unpublished data) has shown that the same phosphorylated dihydroceramides recovered from *P. gingivalis* are also recovered in lipid extracts of carotid endarterectomies from patients with periodontitis. The carotid atheromas were consistently contaminated with bacterial lipids most likely derived from *P. gingivalis* or other phylogenetically-related organisms, as determined by the recovery of 3-OH *iso*$C_{17:0}$ or isobranched 19-carbon long-chain bases. If *P. gingivalis* lipids containing 3-OH *iso*$C_{17:0}$ can contaminate the periodontal tissues [24], local host monocytes and macrophages could incorporate them into their membranes, re-enter the systemic circulation, and transport them to arterial endothelia susceptible to atherosclerosis. Conversely, if *P. gingivalis* gains entry to the systemic circulation during frequent bacteremias associated with oral hygiene measures or oral function, circulating phagocytic cells can clear the microorganism, but will ultimately become contaminated with the bacterial lipids which are likely difficult to break down. Since evidence has demonstrated that the bacterial lipids of *P. gingivalis* are potent activators of proinflammatory events in fibroblasts and peripheral blood monocytes [29], an increased source of inflammatory mediators may be available for the initiation and possible accelerated formation of atherosclerosis.

OBJECTIVE

The purpose of this investigation is to determine whether bacterial ceramides from *P. gingivalis*, when injected into the peritoneum, can induce and/or accelerate the formation of atherosclerosis in C57BL/6J female mice fed either normal or high-fat diets. The total lipid recovered from *P. gingivalis* and two biologically active HPLC lipid fractions will be tested. The biological activity of lipid fractions was previously determined by showing elevated prostaglandin secretion from cultured human gingival fibroblasts in response to IL-1 [29]. All test mice injected with bacterial lipid, regardless of diet, will be compared to control mice without any intra-peritoneal introduction of bacterial lipid. After following the mice for several months on their respective diets, the animals will be sacrificed, and their hearts and aortas removed. Histological cross-sections of the proximal aortas will be stained and examined by light microscopy for extent and severity of atherosclerosis formation. The percent of the aortic wall stained for lipid deposits will be compared among the groups. Additionally, bacterial lipid recovery from the descending aortas will be analyzed using previously described GC-MS methods [24].

MATERIALS AND METHODS

Lipid extraction from *P. gingivalis*

Porphyromonas gingivalis, obtained from ATCC (#33277, type strain), was cultured in an anaerobic chamber as previously described [24]. Extraction of the lipid from *P. gingivalis* was performed according to a Garbus modification [73] of a standardized procedure as described by Bligh and Dyer [74]. A methanol-chloroform solution and water (2:1, vol/vol) was added to the bacterial sample for extraction and allowed to stand overnight. Following this, chloroform ($CHCl_3$) and 2M KCl + 0.5M K_2HPO_4 were added to the sample and vortexed. The lower lipid phase was removed, dried under nitrogen, and after redissolving the lipid extract in chloroform, a small sample was dried and weighed on a microbalance scale. The total lipid extract was then stored at -20^0C until further use.

Lipid fractionation by HPLC

Fractionation of the bacterial lipids by high-performance liquid chromatography (HPLC) was accomplished using a direct phase semipreparative silica gel column (0.5 x 30 cm; silica gel, Supelco Inc.) as previously described [24]. Lipid samples were dissolved in solvent A (hexane-isopropanol-water, 6:8:0.75, vol/vol/vol) to a concentration of 250 mg/5 ml. Approximately 500 µl of the lipid sample was then applied to the column and samples were eluted at 2 ml/min with 1 min fractions collected. The

fractions were then dried under nitrogen and suspended in 2 ml of chloroform. Lipid recovery was determined by weighing a defined amount of each fraction (generally 5 µl dried onto a weighing boat) on a microbalance scale.

Determination of biological activity with human gingival fibroblasts

Primary cultures of human gingival fibroblasts (HGF) previously obtained at the University of Connecticut Health Center Periodontology Clinic during periodontal surgery from healthy sites were used for evaluation of biological activity of the *P. gingivalis* lipid fractions [29]. All cell culturing was performed by the techniques described by Richards and Rutherford [75]. The fibroblasts were cultured in Minimum Essential Medium (MEM) supplemented with 10% fetal calf serum, amphotericin B (1.25 µg/ml), penicillin G (500 U/ml), and streptomycin (500 µg/ml) in a water-saturated, 5% CO_2 atmosphere at 37^0C. For all passaging of cells, fibroblasts were diluted approximately 1:4 with each passage. Cells were harvested using trypsin (0.1%, w/vol) in Ca^{2+}/Mg^{2+}-free phosphate-buffered saline (PBS) and resuspended in MEM for passaging.

Predetermined amounts of selected HPLC lipid fractions were dissolved in $CHCl_3$, transferred to clean conical vials, and dried under nitrogen gas. Since the bacterial lipids showed little solubility in aqueous solvent, the selected fractions were dissolved in ethanol to a 1 mg/ml concentration. Ten µl of each lipid sample was then placed into a 35 mm diameter culture well under a laminar flow hood. Vehicle wells received ethanol only. The ethanol was allowed to evaporate overnight leaving a residue of lipid on the well surface.

The cultured fibroblasts were then inoculated into the culture wells at the same cell number:surface area ratio as was achieved in the culture flasks with cells at confluence. Following inoculation, the fibroblasts were allowed to adhere for 2 hours after which the medium was supplemented with either control medium or medium containing recombinant human IL-1β to a final concentration of 10 ng/ml. After the cells were incubated for another 24 hours, they were examined by light microscopy and photographed.

Prostaglandin recovery in medium samples was determined using stable isotope dilution with deuterated prostaglandin standards. $PGF_{2\alpha}$, 6-keto $PGF_{1\alpha}$, and PGE_2 were quantified in medium samples using a modification of the method of Luderer et al. [76], previously described by Nichols [24]. Each medium sample was supplemented with 100 ng of D_4- $PGF_{2\alpha}$, D_4-6-keto $PGF_{1\alpha}$, and D_4- PGE_2. The fibroblast medium samples were then thawed and the pH adjusted to 3.5 with concentrated formic acid. The acidified medium samples were then applied to reverse phase preparative columns (Supelcoclean, C-18 SPE tubes, 6 ml, Supelco Inc., Bellefonte, PA) mounted on a vacuum manifold. Before applying the medium samples, the C-18 columns (3 ml) were regenerated by running sequentially 3 ml of 100% methanol followed by 3 ml of Ca^{2+}/Mg^{2+}-free PBS (pH 3.5). Each acidified medium sample was then applied to individual C-18 columns, the columns were washed with 3 ml of 25% methanol in water, and enriched prostaglandins were eluted with 3 ml of 100% methanol. The resultant samples were then supplemented with 2 ml of 1% formic acid in water and the prostaglandins were extracted twice with 2 ml of chloroform. The chloroform extracts were dried under nitrogen.

All derivatizing agents were obtained from Pierce Chemical Corp. (Rockford, IL.). Prostaglandin samples were derivatized using the method of Waddell et al. [77]. Briefly, prostaglandin samples were first treated with 30 µl of 2% methoxylamine hydrochloride in pyridine. After standing overnight at room temperature, the samples were dried under nitrogen, dissolved in 30 µl acetonitrile, and treated with both 10 µl pentafluorobenzyl bromide (35% vol/vol in acetonitrile) and 10 µl diisopropylethylamine. The samples were then vortexed, incubated for 20 minutes at 40^0C, and evaporated under nitrogen.

Ceramide analysis by GC-MS

Verification of the presence of the biologically active ceramides [29] in the HPLC lipid fractions was accomplished using gas chromatography-mass spectrometry (GC-MS) analysis according to the method proposed by Nichols [24]. All analyses were performed on a Hewlett Packard 5890 gas chromatograph interfaced with a 5988A mass spectrometer. The *P. gingivalis* fatty acid samples were treated with 50 µl N,O-bis (trimethylsilyl)-trifluoroacetamide (BSTFA) for 4-5 days at room temperature to form trimethylsilyl (TMS) derivatives; and each sample was transferred to a microvial and sealed with a Teflon-lined crimp cap. Each sample was then run on a SBP-1 column (0.1 mm film x 0.25 mm x 15 m) with the inlet block at 310^0C using the splitless mode with a temperature program of 10^0C/min from 200^0C to 300^0C followed by 5^0C/min to 310^0C and 4 min at 310^0C. An electron impact ionization mode was used for the mass

spectrometer with the ion source temperature at 200^{0}C, electron energy at 70 eV, and emission current at 300 mA.

Pooling and purification of biologically active HPLC lipid fractions

HPLC lipid fractions 15-20 and 31-34 were dissolved in 4 ml chloroform sequentially and combined. The pooled fractions were refractionated using HPLC as described above on the same semi-preparative silica gel column (0.5 x 30 cm; silica gel) and eluted in solvent A at 2 ml/min with 1 minute fractions collected. An aliquot from each fraction was dissolved in BSTFA and the solutions were allowed to stand for 1 hour at 60^{0}C. After drying each fraction under nitrogen gas, a small amount of each fraction was evaluated to verify ceramide content using positive-ion GC-MS on a SBP-1 column (0.1 mm film x 0.25 mm x 15 m) as described above.

Animal experiments

A total of 40 four-week old C57BL/6J female mice (# 000664, Jackson Laboratory) were used in the present investigation and separated into eight different groups of five mice each. Twenty mice (a contingency of four groups) were fed a normal diet (LM-485, Harlan Teklad); and the remaining twenty mice (a second contingency of four groups) were fed a high-fat diet (TD 94059, Harlan Teklad) for the entirety of the experiment. This diet, a modification of the Paigen diet [57] by excluding cholic acid, consists of about 4 kcal/g, and contains 1.25% cholesterol and approximately 15% fat.

Cholic acid is normally added to the high fat diet to increase systemic inflammation and accelerate fatty deposition in artery walls. This supplement was removed from the mouse chow so that systemic inflammatory changes were minimized. After a few days of acclimation, each group of the normal diet contingency and each group of the high-fat diet contingency received one of the following via intraperitoneal (*i.p.*) injection:

1. Fraction 17 (10 µl, 1 µg/µl in 100% ethanol) of the previously characterized, biologically-active ceramide HPLC lipid fractions recovered from *P. gingivalis*.
2. Fraction 28 (25 µl, 0.4 µg/µl in 70% ethanol) of the previously characterized, biologically-active ceramide HPLC lipid fractions recovered from *P. gingivalis*.
3. Total lipid (10 µl, 1 µg/µl in 100% ethanol) recovered from *P. gingivalis*.
4. Vehicle control (10 µl 70% ethanol).

Each animal was injected once with its respective solution using a Valco precision sampling syringe (Series C-160, Supelco Inc., Bellefonte, PA), and monitored for changes in activity. Within the first few days after injections, 18 mice died, most of which were in the bacterial lipid groups. Since a significant percentage died so early in the experiment, it was decided to modify the protocol and include additional mice injected with a smaller dose (2.5 µg) of the fraction 28 lipid and the total lipid extract from *P. gingivalis*. Twenty additional female C57BL/6J mice were separated into two contingencies of ten mice each depending on their diet. Each contingency was divided into two groups of five mice each and the following was injected once into the peritoneum per group:

1. Fraction 28 (2.5 µl, 0.1 µg/µl in 100% ethanol) of the previously characterized, biologically-active ceramide HPLC lipid fractions recovered from *P. gingivalis*.
2. Total lipid (2.5 µl, 2.5 µg/µl in 100% ethanol) recovered from *P. gingivalis*.

The mice were housed in cages separated according to group and diet. All experimental methods were approved by both the Center for Laboratory Animal Care (CLAC), and the Animal Care Committee (ACC) at the University of Connecticut Health Center. Furthermore, all animal treatment was performed in a humane manner. The cages were maintained daily for adequate food, water, and bedding by the CLAC staff. The mice were monitored daily for the first two weeks, and then weekly for the remainder of the experiment by the primary investigator for changes in activity, movement, and possible death.

Animal sacrifice, tissue preparation, and staining

The mice were sacrificed after 12-13 weeks on their respective diets. After weighing, each mouse was placed in a closed chamber, anesthetized, and killed by inhalation of carbon dioxide. Immediately after death, dissection and fixation of the appropriate tissues was performed. After opening the chest and abdomen, the heart and aortic tree were exposed and identified. The descending aorta was then cut at the level of the kidneys. Next, the heart and aortic tree were perfused using a 25-gauge needle with Ca^{2+}/Mg^{2+}-free PBS (pH 7.4) until no blood was noted exiting the aorta. Immediately

after perfusion, the descending aortas were cut at the level of the aortic arch, removed, and frozen for further analysis. Next, the hearts were removed from the body, oriented, and cut about halfway through their length at a plane parallel to the tips of the atria with tissue scissors as described by Paigen et al. [57]. This plane allowed for proper orientation of the aortic sinus for cryostat sectioning. The hearts were fixed in 10% formalin and stored overnight in preparation for embedding and freezing.

Following fixation, each heart specimen was examined under a dissecting microscope for proper orientation, and extraneous tissue carefully removed. If needed, adjustments to the orientation of the plane were made at this time with a sharp razor blade. Each heart was then embedded in 16 x 12 x 5 mm blocks containing Tissue Freezing Medium (Triangle Biomedical Sciences), immediately frozen in isopentane cooled on dry ice, and stored at -40^{0}C for further use. Microtomy was performed using a Reichert HistoStat cryostat microtome. In detail, each block was frozen on a cryostat mount with Tissue Freezing Medium, trimmed, and sectioned starting with the most apical portion of the heart. Sequential 10 µm sections were made until the three aortic valve leaflets were located. Once this area was found, serial sections were cut and mounted on Superfrost Plus microscope slides (Fisher Scientific) until the aorta assumed a round shape (just beyond the branch points of the coronary arteries). Since this distance is approximately 280 µm [57], a maximum of about 28 sections per heart were saved.

The sections were then stained as described by Humason [78]. Briefly, slides were rinsed in distilled water and washed in 100% propylene glycol for 5 minutes. Next, they were stained with filtered Oil red O (0.5 g/100 ml propylene glycol) for 15 minutes, and washed in 85% propylene glycol for 5 minutes. After rinsing in several changes of

distilled water, the slides were counterstained with 0.1% Mayer's hematoxylin (Sigma) for 8 minutes. Finally, they were rinsed again in several changes of distilled water and immediately cover-slipped using glycerin-gelatin mounting medium. All slides were allowed to dry overnight.

Quantification of atherosclerotic lesions

All sections were examined on a Leitz Orthoplan light microscope at 4x magnification and photographed with a Nikon CoolPix 5000 digital camera (2560 x 1920 pixels) using a calibrated lens setting. Four sections from each aorta were then used for morphometric evaluation as previously described [79]. Those sections chosen for analysis were from the following aortic regions: the aortic valve leaflets seen in their entirety, the valve attachment sites near the coronary ostia, the valve attachment sites visible as small nodules, and the proximal aorta characterized by its round cross section. Lesion sizes at each of the four sites were quantified, and a mean was calculated to represent the percentage of atherosclerosis formation for each mouse. If aortic regions were not available in some specimens due to sectioning or staining error, no substitutions with other sections were permitted. The extent of atherosclerosis was quantified by computer-assisted image analysis using Adobe Photoshop software. Specifically, the percentage of stained lesion area in the entire vessel wall was calculated by dividing the number of red pixels (of a defined threshold range) by the total number of pixels in the aortic wall.

Lipid recovery from descending aortas

Bacterial lipid extraction of the unfixed descending aorta specimens was performed using a chloroform-methanol solution with water (2:1, vol/vol) as described above. After allowing the specimens to stand for several days in extraction solution, $CHCl_3$ and 2M KCl + 0.5M K_2HPO_4 were added to the samples and vortexed. The lower lipid phase was separated and dried under nitrogen. The lipid extracts were then supplemented with 3 μg of $C_{19:0}$ internal standard, and hydrolyzed for 2 hours in 4N KOH at 100^0C. The samples were then acidified (200 μl of concentrated HCl) and extracted with chloroform (3 x 2 ml). The extracted lipids were dried under nitrogen and treated to form pentafluorobenzyl ester, TMS ether derivatives. Samples were dissolved in 30 μl acetonitrile to which 10 μl of 35% pentafluorobenzyl bromide in acetonitrile and 10 μl of diisopropylethylamine were added. The samples were vortexed and incubated at 40^0C for 20 minutes. After drying the samples under nitrogen, each sample was treated with 40 μl of BSTFA and incubated overnight. Samples were then analyzed using electron-capture negative chemical ionization GC-MS for recovery of 3-OH *iso*$C_{17:0}$ as previously described [24].

Statistical analysis

The stained aortic regions were analyzed by using analysis of variance (ANOVA), comparing injected solution with animal diet (normal chow vs. high-fat chow). In

addition, a similar analysis was performed for the recovered 3-OH *iso*$C_{17:0}$ profiles. All analyses were performed using a computer software package (StatView).

RESULTS

Immediately following the intraperitoneal injections, the majority of the mice experienced limited mobility. After the first week, a few continued to exhibit slow movement, but resumed normal locomotion soon thereafter. However, after three days, 12 deaths had occurred, and an additional six by the end of the first week. Of those 18 mice, the following number died per group: 8 of the total lipid group, 2 of the HPLC fraction 17 group, 6 of the HPLC fraction 28 group, and 2 of the vehicle control group. No other mice succumbed following the initial week. Since 45% of the experimental mice died, including all of those in the total lipid group on the high-fat diet, twenty more female C57BL/6J mice were added to the experiment. These were only injected with fraction 28 and the total lipid extract, but with one-fourth the concentration of the initial dosage. Just as with the higher dose, most of the mice experienced decreased mobility immediately after *i.p.* introduction of the lipid solution. Within the first three days after injections with this lower dose, three mice died. At the end of the first week, a total of 6 mice had died, all in the total lipid groups, regardless of diet. None died in the fraction 28 groups. All of the mice that died appeared weak, lethargic, and exhibited compromised mobility. The remaining mice recovered and seemed active for the remainder of the experiment. All deaths per group are shown in Figure 1.

Figure 2 illustrates the mean body weights of all groups prior to sacrifice. The average weight of the 4-week old female C57BL/6J mice at the start of the experiment was 14.3 g. After 12-13 weeks, the mean weight was 21.0 g for the mice fed the normal diet, and 26.7 g for those fed the high-fat diet. This represents a 46.9% and 86.7%

increase in total body weight, respectively. The 5.7 g (27.1%) difference between the two diet groups was statistically significant ($P < 0.001$). Two-way ANOVA showed no significant difference in weight between any of the lipid treatments and the vehicle control, regardless of diet group. Furthermore, there were no statistically significant differences between the lipid treatments on mouse body weight for either diet group ($P < 0.01$).

In the cross-sectional histomorphometric analysis of atheroma lesions, two aortas in the high-fat diet contingency were discarded due to technical errors: one in the vehicle control group, and the other in the fraction 17 group. All four representatives of the required artery sections were located in 25% of the aortas. Three sections were used in 50% of the aortas; and one or two sections in the remaining 25% of the aortas analyzed. Figures 3 and 4 illustrate the steps taken for analysis with all four section representatives in one of the aortas from a mouse injected with 2.5 μg of the total lipid extract and fed normal chow. Figure 3 shows the original micrographs of the four representative sections at 4x magnification. Stained adipose tissue is noticeable in the tissues surrounding the aortic cross-sections. Figure 4 shows one of the sections digitally outlined, including a higher magnification of a portion of that section with bright red digitally added to all areas of lipid stain within the arterial wall (Panel D). Highlighting the stained areas (seen in Panel C) one particular color facilitated determination of the exact number of pixels for the analysis.

The percent lipid deposition in the arterial wall per group (as determined by pixel counts), is shown in Figure 5. The extent of atherosclerosis in all of the mice was primarily type I and II lesions, namely foam cell and fatty streak formation. In none of

the sections were well-defined acellular lipid cores noticeable. One-way ANOVA showed no difference between diet groups and amount of lipid deposition. However, there was a significant ($P < 0.0001$) difference between bacterial lipid treatments and aortic lipid deposition, regardless of diet. All high-dose lipid treatments were significantly ($P < 0.001$) increased compared to the vehicle control. In fact, a 4.5-fold increase in aortic lipid deposition was noted for all 10 μg lipid groups compared to the vehicle control. For the lower lipid dose (2.5 μg), though, only the total lipid extract group had significantly ($P < 0.001$) more lipid deposits than the vehicle control. Here, when compared with vehicle controls, the amount of lipid stain was doubled for the 2.5 μg fraction 28 group; and was tripled for the 2.5 μg total lipid extract group.

When comparing each treatment group, the mice injected with the higher lipid doses had significantly ($P < 0.001$) more aortic lipid deposits than those injected with the lower doses. In the 10 μg dose, there was no significant difference between fraction 28 and the total lipid extract for aortic lipid deposition, but fraction 17 had significantly ($P < 0.001$) fewer deposits than both fraction 28 and the total lipid extract. For the 2.5 μg dose, there was no statistically significant difference between fraction 28 and the total lipid extract.

For mice fed the normal chow, there was a statistically significant ($P < 0.001$) increase in aortic lipid deposition among all bacterial lipid treatments compared to the vehicle control for the larger lipid dosage. For mice injected with the lower (2.5 μg) lipid dosage, only the total lipid extract showed significantly more deposition than the vehicle control. The mice injected with the higher bacterial lipid doses had significantly ($P < 0.0001$) more deposits than those injected with the lower doses. For mice injected with 10

μg of lipid, there were no statistically significant differences between fractions 17 and 28, and fraction 28 and the total lipid extract. However, there was a significant difference ($P < 0.001$) between fraction 17 and the total lipid extract. In the 2.5 μg dose groups, no difference was noted between fraction 28 and the total lipid extract.

For mice fed the high-fat diet, there was a statistically significant ($P < 0.0001$) increase in aortic lipid deposition among all lipid treatments compared to the vehicle control, regardless of bacterial lipid dosage. The mice injected with the higher lipid doses had significantly ($P < 0.001$) more deposits than those injected with the lower doses. For mice injected with 10 μg of lipid, fraction 28 showed significantly ($P < 0.001$) more lipid deposition than fraction 17. In the 2.5 μg dose groups, the total lipid extract was significantly ($P < 0.001$) greater than fraction 28 lipid.

The descending aortas were analyzed by GC-MS for 3-OH $C_{14:0}$, 3-OH $C_{16:0}$, and 3-OH *iso*$C_{17:0}$ content using a 3-OH $C_{19:0}$ internal standard. Only data for 3-OH *iso*$C_{17:0}$ are shown in Figure 6. There was no statistically significant difference between the two diet groups for recovery of 3-OH *iso*$C_{17:0}$. For the groups injected with 10 μg of lipid, there was a trend of increased 3-OH *iso*$C_{17:0}$ recovery for mice fed high-fat diets; however, in mice on the normal chow, only the total lipid group showed a higher 3-OH *iso*$C_{17:0}$ abundance compared to the other treatment groups. None of these differences were significant using two-way ANOVA. In the mice injected with 2.5 μg of lipid, the 3-OH *iso*$C_{17:0}$ recovery decreased from fraction 28 to the total lipid extract in both diet contingencies, although this was also not statistically significant.

DISCUSSION

Central to the findings of this study are the nature of specific lipids which were administered. As stated previously, more than 50% of the hydroxy fatty acid content of *P. gingivalis* is 3-OH *iso*$C_{17:0}$, none of which is known to be produced by mammalian species. Previous studies have recovered ceramides of unknown structures containing 3-OH *iso*$C_{17:0}$ from diseased human gingival tissues, cementum, and carotid endarterectomies [27, 72]. Furthermore, only the *Bacteroides* species found in humans are capable of producing such lipids. Since several of these species have been associated with periodontal attachment loss, the recovery of 3-OH *iso*$C_{17:0}$ within human vascular tissues suggests the possibility that periodontal infection may contribute to cardiovascular diseases such as atherosclerosis, ischemic heart disease, myocardial infarction, and stroke.

Mass spectrometry and nuclear magnetic resonance have elucidated the structures of the two complex ceramide HPLC lipid fractions used in this study [28]. Fraction 17 lipids (Figure 7) have three aliphatic constituents: an *iso*$C_{15:0}$ chain that is ester-linked to the β carbon of the 3-OH *iso*$C_{17:0}$; and either *iso*$C_{17:0}$, $C_{18:0}$, or *iso*$C_{19:0}$ long-chain bases in amide linkage to the 3-OH *iso*$C_{17:0}$. Attached to the first carbon of the long-chain bases is a phosphoglycerol head group with a total lipid mass of 933, 947, or 961 amu, as detected by electrospray MS analysis. Loss of the phosphorylated head group of fraction 17 lipids occurs from thermal decomposition associated with the injection block exposure under GC-MS analysis. This results in loss of the *iso*$C_{15:0}$ chain, desaturation of the proximal end of the long-chain base, and formation of McLafferty ions, creating

structures with long-chain bases in imine linkage to 3-OH *iso*$C_{17:0}$ with masses of 577, 591, or 605 amu.

Fraction 28 lipids (Figure 8) have three long-chain bases in amide linkage to 3-OH *iso*$C_{17:0}$. As with fraction 17 lipids, one aliphatic chain represents 3-OH *iso*$C_{17:0}$ while the others are either *iso*$C_{17:0}$, $C_{18:0}$, or *iso*$C_{19:0}$ long-chain bases. When the phosphoethanolamine head group is attached to the first carbon of the long-chain base, the mass of this ceramide lipid is 678, 692, or 706 amu. Under GC-MS analysis conditions, fraction 28 lipids also undergo thermal decomposition with loss of the phosphorylated head group that produces structures with masses of 667, 681 and 695 amu.

The concept of infection as a cause of atherosclerosis is not new to cardiovascular pathology. Thus far, researchers have suggested *Chlamydia pneumoniae* [80], *Helicobacter pylori* [81], and cytomegalovirus [82] as possible infectious links between systemic infection and cardiovascular disease. Of these, the largest body of evidence supports infection with *C. pneumonia*, which has been detected in up to 80% of atherosclerotic vessels [83]. Furthermore, viable *C. pneumonia* has been recovered from 38.5% of aortic aneurysms in another study [84]. Although *H. pylori* and cytomegalovirus have been discovered in atheromatous vessels by DNA analyses, their association is much weaker [85]. Most recently, periodontal pathogens such as *P. gingivalis*, *P. intermedia*, *T. forsythensis*, and *A. actinomycetemcomitans*, have been recovered from 44% of atheromas by PCR analysis of 16s ribosomal DNA [86].

Several mechanisms have been proposed for the role of infection as a causative agent of cardiovascular diseases, especially atherosclerosis. The evidence accumulated

thus far suggests the possibility that microorganisms can directly invade vascular endothelial cells, initiating a local inflammatory response. With the frequent bacteremias associated in patients with periodontitis, it is certainly possible for specific pathogens such as *P. gingivalis* to attach to vascular endothelium just as they would the junctional or sulcular epithelial cells in a periodontal pocket. In fact, researchers have found *in vitro* evidence of *P. gingivalis* invasion of both bovine aortic endothelial cells [70] and, more recently, human carotid and coronary endothelium [87]. Second, microorganisms may enhance atherogenesis by recruiting host inflammatory cells, stimulating pro-inflammatory cytokines production by the endothelial cells, or upregulating macrophage oxLDL receptors. Third, inflammatory cytokines produced from local sources, such as the periodontal pocket, may enter the systemic circulation, finding their way to vascular walls.

Assuming this potential of bacterial infection as a contributing agent for atherosclerosis, Li and colleagues [88] intravenously inoculated heterozygous ApoE deficient and wild-type C57BL/6 mice with live *P. gingivalis* weekly for 10, 14, or 24 weeks. Both cross-sectional and en-face quantification of aortic atheroma formation showed a statistically significant 7-fold increase of lesion area in the transgenic mice at 14 weeks on a normal diet compared to controls on normal chow. The wild-type mice only had early foam cell lesions after 24 weeks when fed a high-fat diet. Furthermore, *P. gingivalis* 16s ribosomal DNA was found only after 24 weeks in all samples injected with the bacterium. Lalla and coworkers [89] applied *P. gingivalis* topically in the oral cavity of homozygous ApoE deficient mice over a 3-week period. After 17 weeks, the hearts and proximal aortas of the $ApoE^{-/-}$ mice showed a statistically significant 40% increase in

mean atherosclerotic lesion area compared to controls. Interestingly, PCR analysis of the vessel walls showed that only 2 of 9 infected mice were positive for *P. gingivalis* DNA, suggesting that although it may be possible for these microorganisms to invade endothelial cells, it may not be an absolute requirement in order to elicit an inflammatory response. Thus, the entire *P. gingivalis* organism is certainly capable of accelerating atherosclerosis formation in ApoE deficient mice, but it is unclear as to what portion of the bacterium stimulates the inflammatory response.

A fourth proposed mechanism focuses on the specific bacterial lipids used in this experiment. If periodontal pathogens like *P. gingivalis* can readily attach to the epithelial cells in a periodontal pocket [33] or invade the underlying connective tissue [34], they could introduce their cell wall components, some of which contain 3-OH *iso*$C_{17:0}$, to host inflammatory cells such as monocytes and macrophages [24]. With the evidence suggesting that *P. gingivalis* releases outer membrane vesicles in culture medium [30], it is certainly plausible that other cells local to the inflamed gingival connective tissue may incorporate these vesicles into their own membranes. These cells might then re-enter the circulation carrying these biologically active lipids in their cell membranes to other sites including arterial walls. As the monocytes enter the intima, the bacterial lipid can enhance the inflammatory response, thus accelerating the atherogenic process. It is this mechanism that is the basis of this study.

The finding that 15 mice died within the first three days after injection, and 9 more by the end of the first week is significant. Those that died appeared weak with limited movement during that time period, but none had skin lesions at the site of injection. The deaths of two mice in the control group on the high-fat diet are most likely

due to technical error in the injection sequence. This group was injected after the total lipid group on the normal diet. Although the injection syringe was flushed several times with 100% ethanol in between groups, there may have been some residual lipid contamination of the syringe which was introduced into these mice. The highest proportion of deaths per group was in the total lipid group (70%). Eighty percent died after introduction of 10 μg of lipid, and 60% died with the 2.5 μg dose. Of the other groups, only two died after injection with fraction 17, and six with fraction 28 (all of which were with the higher dose). Since the animals died relatively soon after injection, it is unlikely that the difference in diet influenced this finding.

It is unlikely that the *i.p.* use of ethanol as a solvent contributed to the animals' death in this experiment. The mice in this experiment were injected with a single dose of solution ranging from 0.000143 mg/kg to 0.00143 mg/kg. This proportion of alcohol is much less than that used in previous reports which describe its toxicity and systemic effects, and resulted in zero deaths when given via *i.p.* injection [90, 91]. One particular study found a dose-dependent relationship between alcohol concentration by intravenous injection and central nervous depression, but with intraperitoneal administration, the depressant effect of ethanol increased with increasing concentration up to 70%, but showed a significant reduction at 90% [92]. Thus, it appears probable that a 70-100% ethanol concentration at low doses by *i.p.* injection would not induce respiratory depression sufficient enough to kill mice, particularly 3 to 5 days later.

Unpublished necropsy reports 2-3 days after *i.p.* injection of four mice with 5 μg of *P. gingivalis* ceramide lipid in 5 μl of ethanol showed peritonitis and transmural necrotizing enteritis. Interestingly, half of these mice exhibited signs of hepatic necrosis.

Although it is possible that some of these biologically active lipids may have been inadvertently injected into other abdominal organs, such a finding may also suggest that they can be carried to other organ tissues in addition to the vasculature.

The Oil red O stain was chosen because of its popularity with other laboratories describing atherosclerosis formation as determined by light microscopy. Like the Sudan dyes, it is a general stain for lipids that exist as fat globules in cells and tissues. It will only stain lipids that are liquid or semi-liquid at the staining temperature. Thus, those lipids that are solid or crystalline remain unaffected. However, if the lipid is bound to protein or carbohydrate, then even if it is a liquid or semi-liquid, it might not stain. Oil red O can be used with either isopropanol or propylene glycol as a solvent; however, some neutral lipid may be dissolved during the staining process.

In almost every stained section in this study, there were several areas of very bright-red droplets of stain located at many sites throughout the arterial tissue. The difficulty was determining the validity of these stained areas. At some sites, it was unclear as to whether they were true positives for atheromatous lipid, or artifactual findings. In many of the mice fed the high-fat diet, there was much more adipose tissue around the target sections, which provided a larger source of unwanted extraneous stain droplets in the arterial wall which could not be washed away effectively. Furthermore, some sections stained and/or counterstained at different intensities than others. This made the analysis for extent of atheroma formation challenging and provided a possible source of error.

In order to deal with this problem, a protocol was devised for the analysis. The amount of stain per section was determined by selecting all stained areas with a

consistent point sample threshold for all analyzed sections. Red stains which were obvious artifact (unusually large globules, globules impinging on vessel borders, etc.) were excluded; those which were questionable were included in the analysis. Since some sections were stained at different intensities, the manual selection (and de-selection) of stain made the analysis much more precise than solely allowing the computer to select all colors in a defined red range, by which some colors would be either included or excluded from the analysis. Once this was completed, it was relatively easy to calculate the percentage of each stained aortic area: the number of highlighted pixels (Panel D, Figure 4) in the entire aorta was divided by the total number of pixels of the entire outlined section (Panel A, Figure 4).

The majority of the lesions noted in this experiment were stage I and II lesions. Although much of the lipid deposition was found at the aortic valve cusps, many other sections of the aortic sinus and proximal aorta had similar amounts of stain. A few sections from mice fed the high-fat diet had lesions consisting of small pools of lipid deposition. In none of the sections were well-defined borders found, walling off a necrotic core of lipid and foam cells. None of the coronary arteries were occluded or had significantly more intra-vascular lipid deposition that the aortas themselves. The 12-13 week duration of the experiment was probably not sufficient to induce true atheroma formation in these mice. The stage of atherosclerosis seen in this study is consistent with other reports using similar C57BL/6J mice [56, 57, 93, 94].

Although the finding that 10 μg of lipid had a significant (3-4-fold) increase in lipid deposition is important, it is more interesting that the smaller 2.5 μg dose of total lipid extract was associated with a significant increase in fatty streak formation. There

was also a trend toward increased lipid deposition from fractions 17 and 28 to the total lipid extract, although it was not always statistically significant. Since the total lipid extract contains both fractions 17 and 28 (as well as other unreported biologically active ceramides), this finding was not unexpected. Therefore, if all of the mice in the high-fat diet total lipid group had not died, the intra-vascular lipid deposition would probably have been the highest of all the groups.

For mice fed the normal chow, there were no significant differences between 10 μg injections of fractions 17 and 28, and between fraction 28 and the total lipid extract for aortic lipid deposition. Furthermore, fraction 28 and the total lipid extract did not differ significantly between diet groups. Such results suggest that *i.p.* administration of these ceramide lipids to mice fed a normal diet has a similar effect with respect to fatty streak formation as those fed a high-fat diet. In other words, *P. gingivalis* lipids appear to accelerate the rate of atherosclerosis formation in C57BL/6J mice on normal diets. These findings give additional credence to the hypotheses offered by Beck and coworkers [95] and Nichols [24] for the concepts that periodontal inflammatory factors can have an effect on other systemic inflammatory-mediated pathological processes.

After analyzing the abundance of 3-OH *iso*$C_{17:0}$ recovered from the descending aortas, no statistically significant differences were noted among groups. The amount recovered was extremely small compared to what is seen after 3-OH *iso*$C_{17:0}$ extraction from whole cells of *P. gingivalis*. Furthermore, it is much less than the previously reported abundances of the same fatty acid from human carotid endarterectomies [72], although the relative size of the specimens may have accounted for some of the difference. The paucity of 3-OH *iso*$C_{17:0}$ recovered from the aortas may suggest that these

fatty acids may be found in other organ tissues such as the liver, gut, or brain, which is consistent with the necropsy findings. It also suggests that only very small amounts of these ceramides are required to exacerbate intra-vascular inflammatory pathology.

CONCLUSION

Further studies are needed to elucidate this connection between periodontitis and cardiovascular disease. Although it appears that specific bacterial ceramide lipids are as pathogenic as the bacteria themselves, the two need to be compared in a single experiment to confirm this hypothesis. Such a study would help to further understand the overall mechanism of pathogenesis. Are peripheral blood monocytes transporting the lipids to other tissues, or are the inflammatory mediators produced at diseased periodontal tissues entering the systemic circulation and influencing vascular pathogenesis? More mice per group, blood tests for inflammatory mediators, and tests with LPS are needed to draw further conclusions. Additionally, introducing either LPS or these biologically active bacterial lipids in C3H/HeJ mice, which are TLR-4 knockout mice, may further aid in the understanding of the mechanisms of action for both bacterial toxins.

In conclusion, a single intraperitoneal injection of *P. gingivalis* ceramide lipids facilitates increased lipid deposition in the proximal aortic arches of C57BL/6J female mice. Although the two tested HPLC lipid fractions seem to exhibit equivalent responses with respect to atherosclerosis formation, the total lipid extract appears to have a greater influence than either of the two biologically active ceramides when compared to controls. This could mean that fractions 17 and 28 act synergistically, or that other biologically active lipids are present in *P. gingivalis* lipid extracts. Furthermore, the lipids can be recovered from the aortas as evidenced by the recovery of 3-OH *iso*$C_{17:0}$ from the descending aortas. The minute amount recovered, however, suggests the possibility that

these bacterial ceramides may be carried to other tissues. Finally, the early deaths of nearly half of the mice illustrate the potency of these bacterial lipids, and the potential for a systemic hyper-inflammatory condition.

	Vehicle Control	Fraction 17 (10 µg)	Fraction 28 (10 µg)	Total Lipid (10 µg)	Fraction 28 (2.5 µg)	Total Lipid (2.5 µg)
Normal Diet	0/5	2/5	3/5	3/5	0/5	2/5
High-fat Diet	2/5	0/5	3/5	5/5	0/5	4/5
Total Deaths	20%	20%	60%	80%	0%	60%

Figure 1. Number of mice per group that died after a single intraperitoneal injection of each solution. Both 10 µg and 2.5 µg doses are shown.

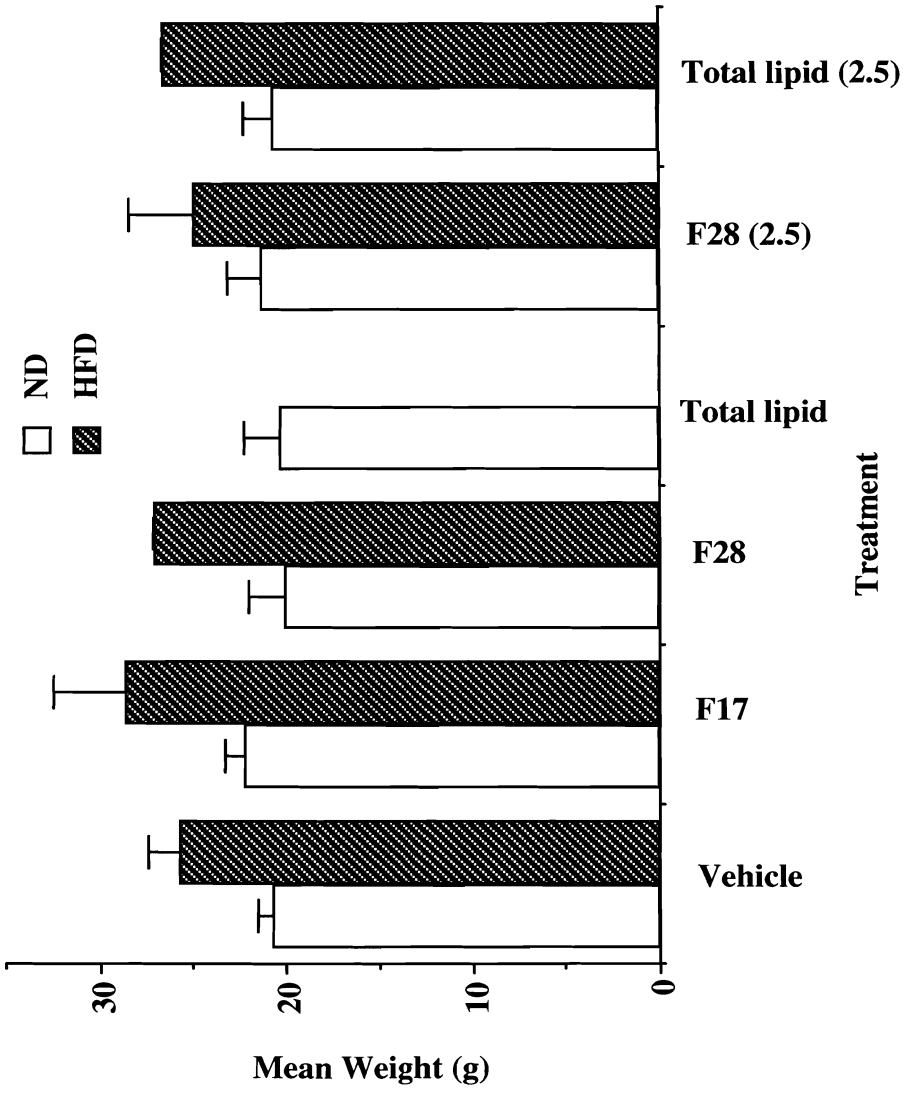

Figure 2. Comparison of final mouse body weights per treatment group fed either normal or high-fat chow. Error bars represent standard deviations.

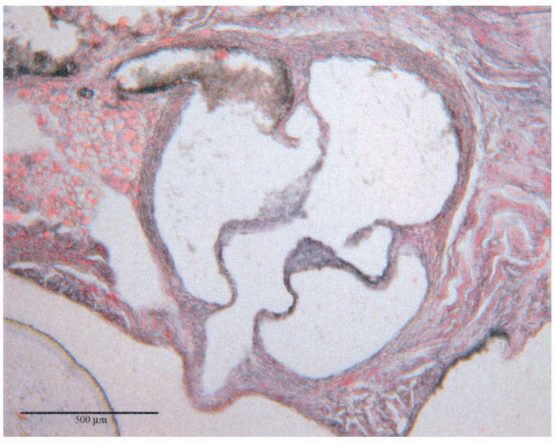

Section A

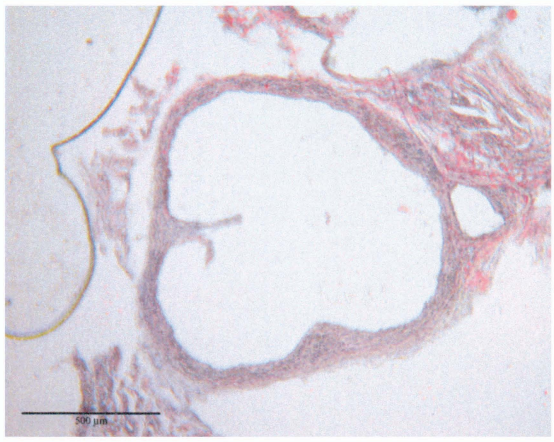

Section B

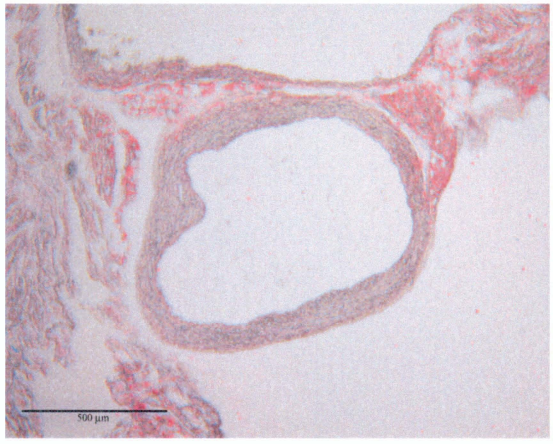

Section C

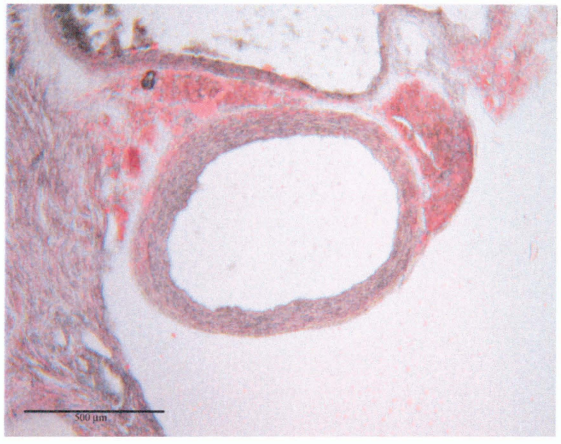

Section D

Figure 3. Representative aortic cross-sections (4x) from a mouse injected with 2.5 µg of the total lipid extract stained with Oil red O and counterstained with Mayer's hematoxylin. Section A shows the aortic valve leaflets in their entirety. Section B shows the valve attachment sites at the level of the coronary artery ostium. Section C shows the valve attachment sites visible as small nodules. Section D shows the proximal aorta characterized by its round cross section. Measure bars represent 500 µm.

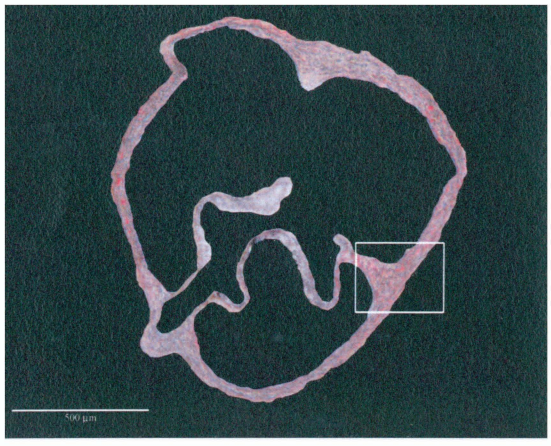

Panel A

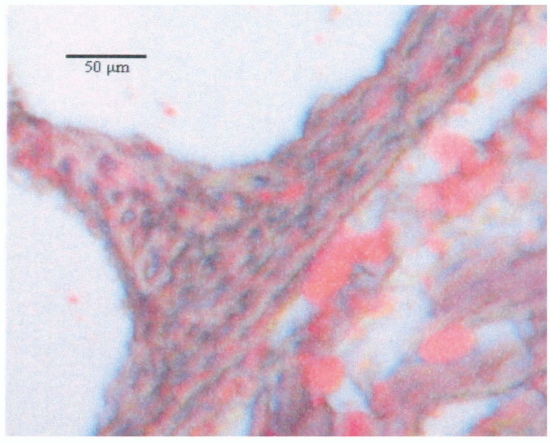

Panel B

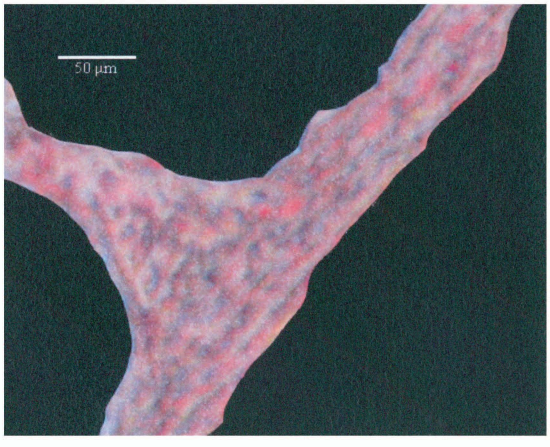

Panel C

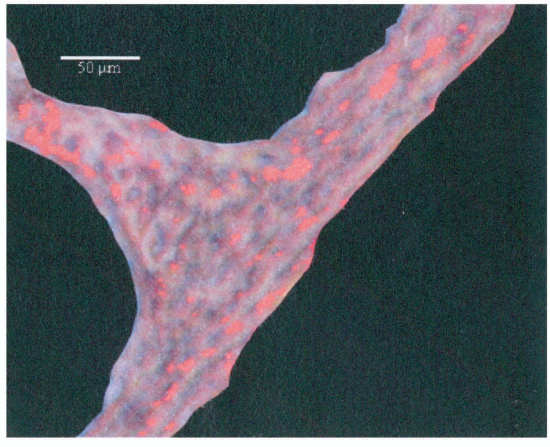

Panel D

Figure 4. Higher magnifications of an aortic cross-section from a mouse injected with 2.5 µg of the total lipid extract illustrating the steps used for analysis. Panel A is a section taken at the level of the aortic valves (4x), but is digitally outlined in black to facilitate analysis. Scale bar represents 500 µm. Panels B, C, and D are digital zooms of the aortic wall shown in the boxed portion of Panel A. Scale bars represent 50 µm. Panel B is from the original micrograph stained with Oil red O and counterstained with Mayer's hematoxylin. Both stained adipose tissue and unwashed red stain can be seen in the surrounding connective tissue. Panel C shows the stained outlined wall. Panel D shows the selected stains digitally highlighted in bright red.

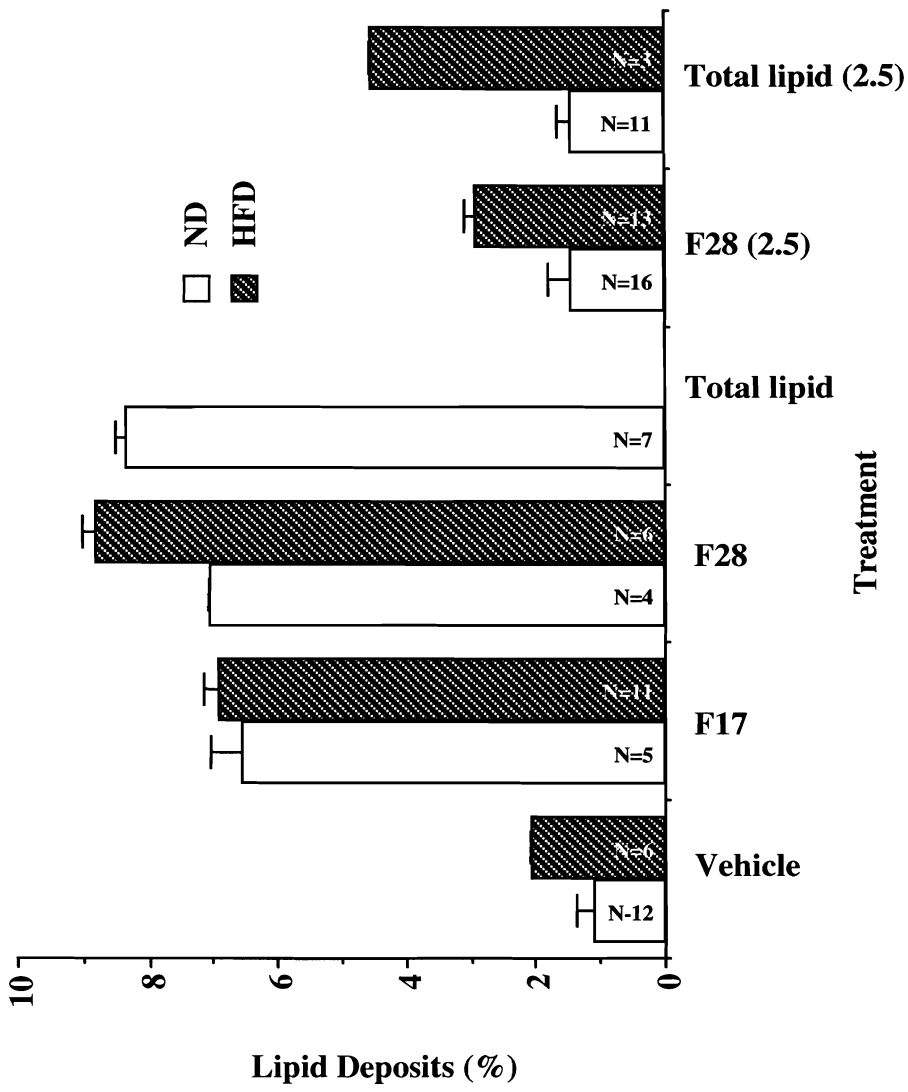

Figure 5. Percent lipid deposits (defined by pixel counts) within the proximal aortic wall per treatment group fed either normal or high-fat chow. The numbers of sections analyzed per group are shown in each of the bars. Error bars represent standard deviations.

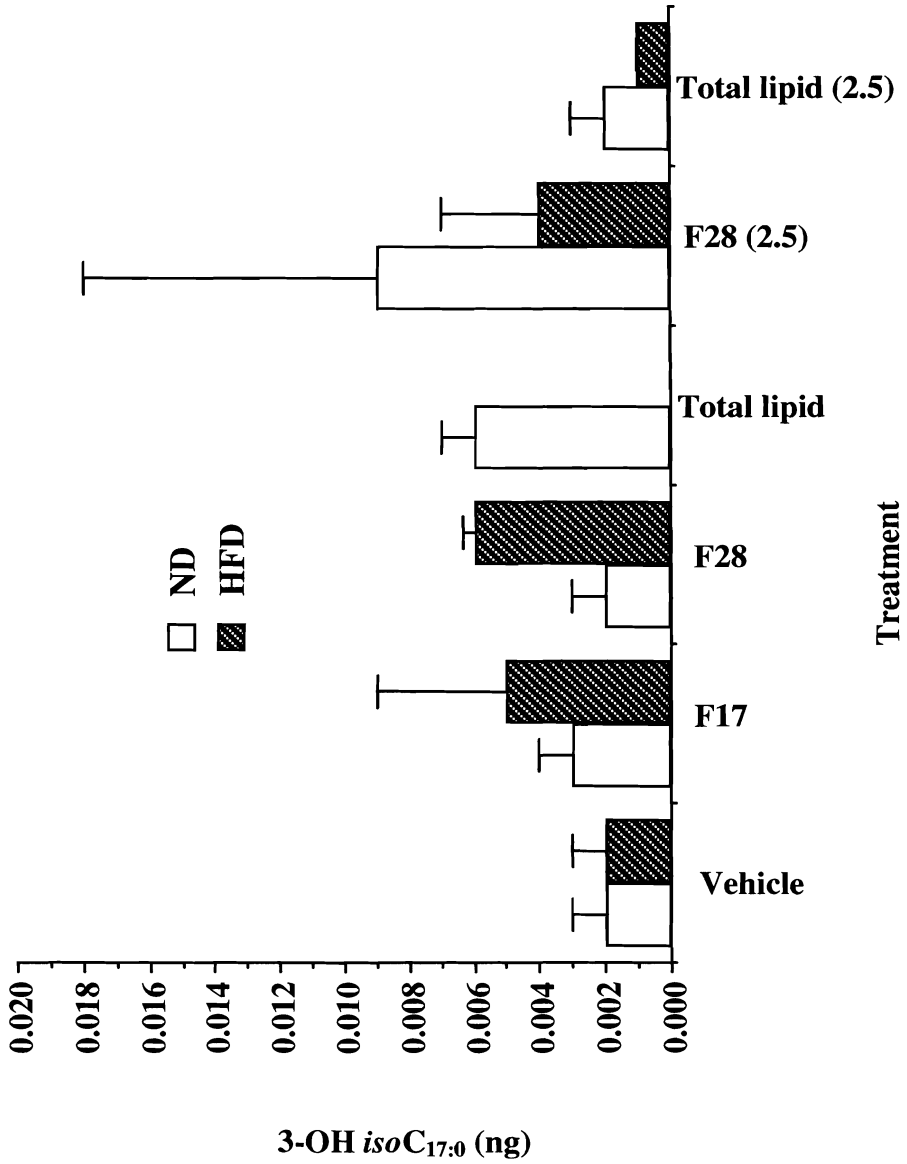

Figure 6. Comparison of 3-OH *iso*$C_{17:0}$ relative abundance recovered from descending aortas per treatment group fed either normal or high-fat chow. Error bars represent standard deviations.

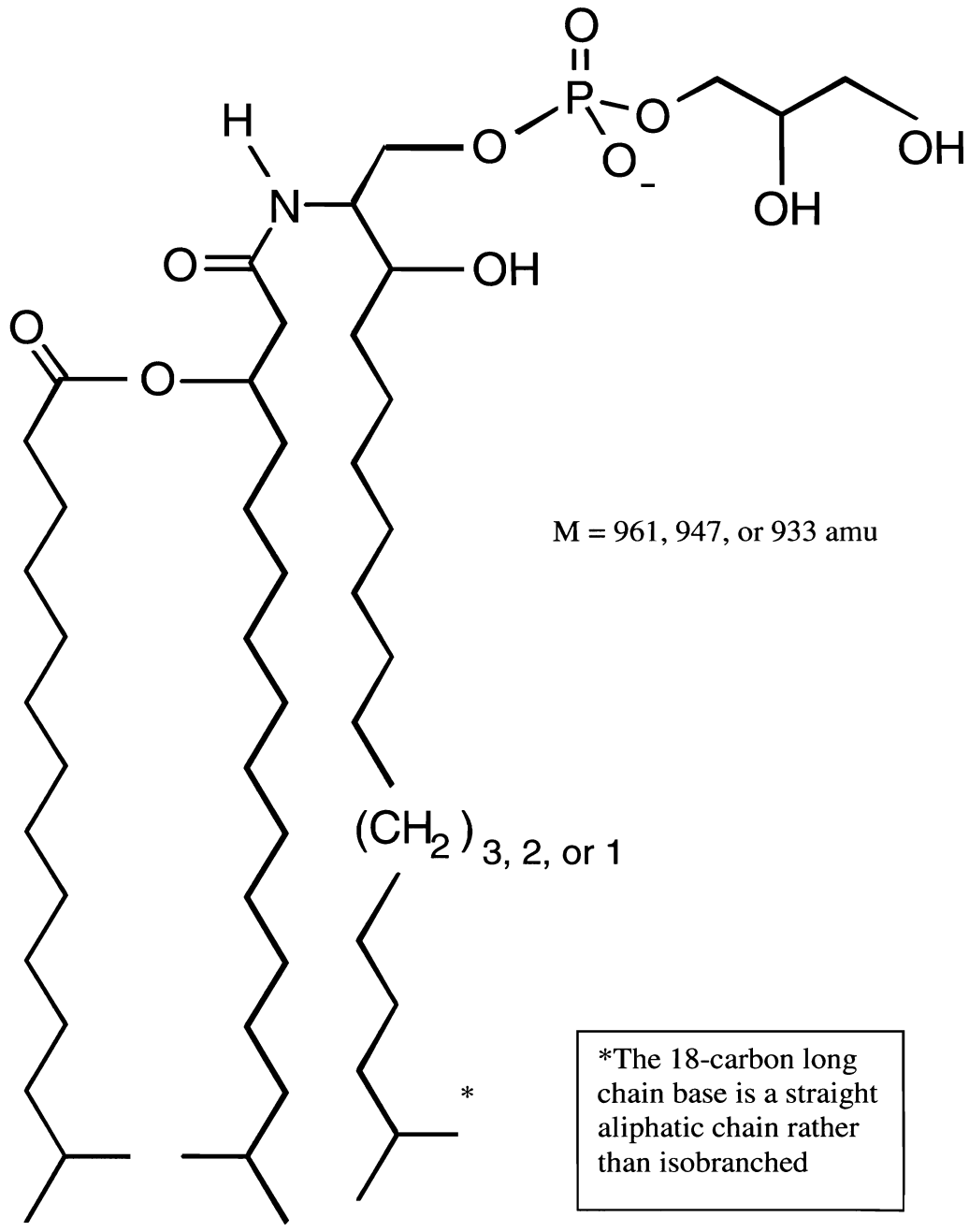

Figure 7. Chemical structure of *Porphyromonas gingivalis* HPLC lipid fraction 17 ceramides. The long-chain base in the middle is 3-OH *iso*$C_{17:0}$. Sodium methoxide treatment releases the 15-carbon isobranched methyl ester on the left. Two of the long-chain bases are amide-linked with an attached phosphoglycerol head group.

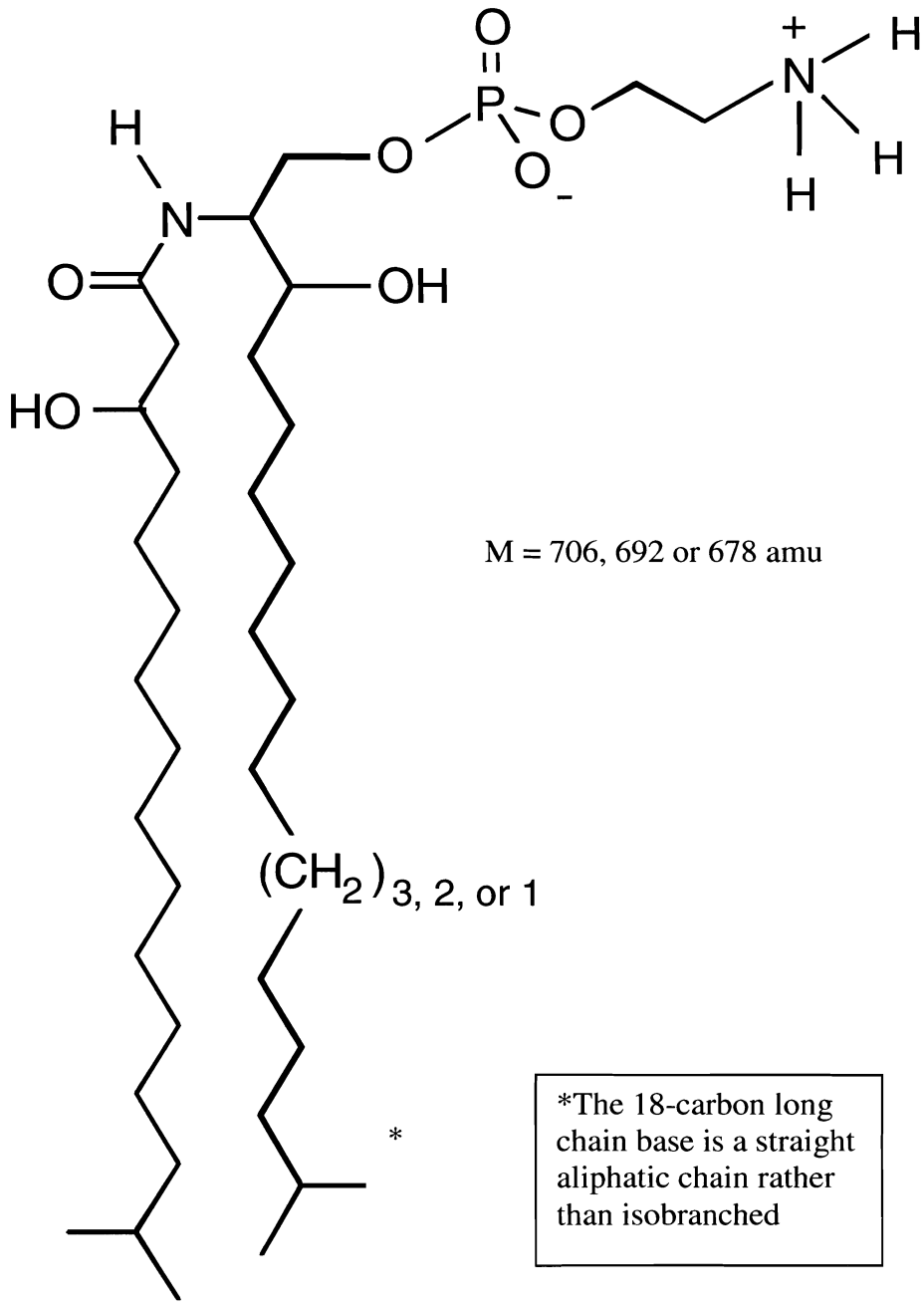

Figure 8. Chemical structure of *Porphyromonas gingivalis* HPLC lipid fraction 28 ceramides. The long-chain base on the left is 3-OH *iso*$C_{17:0}$. The long-chain bases are amide-linked with an attached phosphoethanolamine head group.

REFERENCES

1. Brown, L.J., R.C. Oliver, and H. Löe, *Periodontal diseases in the U.S. in 1981: prevalence, severity, extent, and role in tooth mortality.* J Periodontol, 1989. **60**(7): p. 363-70.
2. Page, R.C. and H.E. Schroeder, *Pathogenesis of inflammatory periodontal disease. A summary of current work.* Lab Invest, 1976. **34**(3): p. 235-49.
3. Listgarten, M.A. and L. Helldén, *Relative distribution of bacteria at clinically healthy and periodontally diseased sites in humans.* J Clin Periodontol, 1978. **5**(2): p. 115-32.
4. Moore, W.E., *Microbiology of periodontal disease.* J Periodontal Res, 1987. **22**(5): p. 335-41.
5. Socransky, S.S., et al., *Microbial complexes in subgingival plaque.* J Clin Periodontol, 1998. **25**(2): p. 134-44.
6. Shiloah, J., et al., *The prevalence of Actinobacillus actinomycetemcomitans, Porphyromonas gingivalis, and Bacteroides forsythus in humans 1 year after 4 randomized treatment modalities.* J Periodontol, 1998. **69**(12): p. 1364-72.
7. Schwartz, J., F.L. Stinson, and R.B. Parker, *The passage of tritiated bacterial endotoxin across intact gingival crevicular epithelium.* J Periodontol, 1972. **43**(5): p. 270-6.
8. Rizzo, A.A., *Absorption of bacterial endotoxin into rabbit gingival pocket tissue.* Periodontics, 1968. **6**(2): p. 65-70.

9. Frank, R.M., *Bacterial penetration in the apical pocket wall of advanced human periodontitis.* J Periodontal Res, 1980. **15**(6): p. 563-73.

10. Sandros, J., et al., *Porphyromonas gingivalis invades human pocket epithelium in vitro.* J Periodontal Res, 1994. **29**(1): p. 62-9.

11. Liakoni, H., P. Barber, and H.N. Newman, *Bacterial penetration of pocket soft tissues in chronic adult and juvenile periodontitis cases. An ultrastructural study.* J Clin Periodontol, 1987. **14**(1): p. 22-8.

12. Kinane, D.F., *Periodontal diseases' contributions to cardiovascular disease: an overview of potential mechanisms.* Ann Periodontol, 1998. **3**(1): p. 142-50.

13. Schumann, R.R., et al., *Structure and function of lipopolysaccharide binding protein.* Science, 1990. **249**(4975): p. 1429-31.

14. Shapira, L., et al., *Porphyromonas gingivalis lipopolysaccharide stimulation of human monocytes: dependence on serum and CD14 receptor.* Oral Microbiol Immunol, 1994. **9**(2): p. 112-7.

15. Medzhitov, R., P. Preston-Hurlburt, and C.A. Janeway, Jr., *A human homologue of the Drosophila Toll protein signals activation of adaptive immunity.* Nature, 1997. **388**(6640): p. 394-7.

16. Ogawa, T., et al., *Bacterial fimbriae activate human peripheral blood monocytes utilizing TLR2, CD14 and CD11a/CD18 as cellular receptors.* Eur J Immunol, 2002. **32**(9): p. 2543-50.

17. Barton, G.M. and R. Medzhitov, *Toll-like receptors and their ligands.* Curr Top Microbiol Immunol, 2002. **270**: p. 81-92.

18. Hirschfeld, M., et al., *Signaling by toll-like receptor 2 and 4 agonists results in differential gene expression in murine macrophages.* Infect Immun, 2001. **69**(3): p. 1477-82.

19. Yoshimura, A., et al., *Lipopolysaccharides from periodontopathic bacteria Porphyromonas gingivalis and Capnocytophaga ochracea are antagonists for human toll-like receptor 4.* Infect Immun, 2002. **70**(1): p. 218-25.

20. Lamont, R.J. and H.F. Jenkinson, *Life below the gum line: pathogenic mechanisms of Porphyromonas gingivalis.* Microbiol Mol Biol Rev, 1998. **62**(4): p. 1244-63.

21. Imamura, T., *The role of gingipains in the pathogenesis of periodontal disease.* J Periodontol, 2003. **74**(1): p. 111-8.

22. Garrison, S.W., S.C. Holt, and F.C. Nichols, *Lipopolysaccharide-stimulated PGE2 release from human monocytes. Comparison of lipopolysaccharides prepared from suspected periodontal pathogens.* J Periodontol, 1988. **59**(10): p. 684-7.

23. Hausmann, E., et al., *Structural requirements for bone resorption by endotoxin and lipoteichoic acid.* J Dent Res, 1975. **54 Spec No B**: p. B94-9.

24. Nichols, F.C., *Novel ceramides recovered from Porphyromonas gingivalis: relationship to adult periodontitis.* J Lipid Res, 1998. **39**(12): p. 2360-72.

25. Johne, B., I. Olsen, and K. Bryn, *Fatty acids and sugars in lipoplysaccharides from Bacteroides intermedius. Bacteroides gingivalis and Bacteroides loescheii.* Oral Microbiol Immunol, 1988. **3**(1): p. 22-7.

26. Mayberry, W.R., *Cellular distribution and linkage of D-(-)-3-hydroxy fatty acids in Bacteroides species.* J Bacteriol, 1980. **144**(1): p. 200-4.

27. Nichols, F.C., *Distribution of 3-hydroxy iC17:0 in subgingival plaque and gingival tissue samples: relationship to adult periodontitis.* Infect Immun, 1994. **62**(9): p. 3753-60.

28. Nichols, F.C., et al., *Structures and biological activity of phosphorylated dihydroceramides of Porphyromonas gingivalis.* J Lipid Res, 2004.

29. Nichols, F.C., et al., *Prostaglandin E2 secretion from gingival fibroblasts treated with interleukin-1beta: effects of lipid extracts from Porphyromonas gingivalis or calculus.* J Periodontal Res, 2001. **36**(3): p. 142-52.

30. Smalley, J.W. and A.J. Birss, *Extracellular vesicle-associated and soluble trypsin-like enzyme fractions of Porphyromonas gingivalis W50.* Oral Microbiol Immunol, 1991. **6**(4): p. 202-8.

31. Lineberger, L.T. and T.J. De Marco, *Evaluation of transient bacteremia following routine periodontal procedures.* J Periodontol, 1973. **44**(12): p. 757-62.

32. Wank, H.A., et al., *A quantitative measurement of bacteremia and its relationship to plaque control.* J Periodontol, 1976. **47**(12): p. 683-6.

33. Deshpande, R.G., M. Khan, and C.A. Genco, *Invasion strategies of the oral pathogen porphyromonas gingivalis: implications for cardiovascular disease.* Invasion Metastasis, 1998. **18**(2): p. 57-69.

34. Saglie, F.R., A. Marfany, and P. Camargo, *Intragingival occurrence of Actinobacillus actinomycetemcomitans and Bacteroides gingivalis in active destructive periodontal lesions.* J Periodontol, 1988. **59**(4): p. 259-65.

35. Dean, R.T. and D.T. Kelly, eds. *Atherosclerosis: Gene Expression, Cell Interactions, and Oxidation.* 2000, Oxford University Press: New York. 450.

36. De Nardin, E., *The role of inflammatory and immunological mediators in periodontitis and cardiovascular disease.* Ann Periodontol, 2001. **6**(1): p. 30-40.

37. Ross, M.H., L.J. Romrell, and G.I. Kaye, *Histology: A Text and Atlas.* 3rd ed. 1995, Baltimore: Williams & Wilkins. 823.

38. Giddens, D.P., C.K. Zarins, and S. Glagov, *The role of fluid mechanics in the localization and detection of atherosclerosis.* J Biomech Eng, 1993. **115**(4B): p. 588-94.

39. Stary, H.C., et al., *A definition of initial, fatty streak, and intermediate lesions of atherosclerosis. A report from the Committee on Vascular Lesions of the Council on Arteriosclerosis, American Heart Association.* Arterioscler Thromb, 1994. **14**(5): p. 840-56.

40. Stary, H.C., et al., *A definition of advanced types of atherosclerotic lesions and a histological classification of atherosclerosis. A report from the Committee on Vascular Lesions of the Council on Arteriosclerosis, American Heart Association.* Arterioscler Thromb Vasc Biol, 1995. **15**(9): p. 1512-31.

41. Noll, G., *Pathogenesis of atherosclerosis: a possible relation to infection.* Atherosclerosis, 1998. **140 Suppl 1**: p. S3-9.

42. Quinn, M.T., et al., *Oxidatively modified low density lipoproteins: a potential role in recruitment and retention of monocyte/macrophages during atherogenesis.* Proc Natl Acad Sci U S A, 1987. **84**(9): p. 2995-8.

43. Navab, M., et al., *Pathogenesis of atherosclerosis.* Am J Cardiol, 1995. **76**(9): p. 18C-23C.

44. Cockerill, G.W., et al., *High-density lipoproteins inhibit cytokine-induced expression of endothelial cell adhesion molecules.* Arterioscler Thromb Vasc Biol, 1995. **15**(11): p. 1987-94.

45. Steinberg, D., *Arterial metabolism of lipoproteins in relation to atherogenesis.* Ann N Y Acad Sci, 1990. **598**: p. 125-35.

46. Boullier, A., et al., *Scavenger receptors, oxidized LDL, and atherosclerosis.* Ann N Y Acad Sci, 2001. **947**: p. 214-22; discussion 222-3.

47. Gerrity, R.G., *The role of the monocyte in atherogenesis: I. Transition of blood-borne monocytes into foam cells in fatty lesions.* Am J Pathol, 1981. **103**(2): p. 181-90.

48. Qi, M., H. Miyakawa, and H.K. Kuramitsu, *Porphyromonas gingivalis induces murine macrophage foam cell formation.* Microb Pathog, 2003. **35**(6): p. 259-67.

49. Miyakawa, H., et al., *Interaction of Porphyromonas gingivalis with low-density lipoproteins: implications for a role for periodontitis in atherosclerosis.* J Periodontal Res, 2004. **39**(1): p. 1-9.

50. Campbell, J.H., et al., *Heparan sulfate-degrading enzymes induce modulation of smooth muscle phenotype.* Exp Cell Res, 1992. **200**(1): p. 156-67.

51. Rabbani, R. and E.J. Topol, *Strategies to achieve coronary arterial plaque stabilization.* Cardiovasc Res, 1999. **41**(2): p. 402-17.

52. Zhang, S.H., et al., *Spontaneous hypercholesterolemia and arterial lesions in mice lacking apolipoprotein E.* Science, 1992. **258**(5081): p. 468-71.

53. Purcell-Huynh, D.A., et al., *Transgenic mice expressing high levels of human apolipoprotein B develop severe atherosclerotic lesions in response to a high-fat diet.* J Clin Invest, 1995. **95**(5): p. 2246-57.

54. Ishibashi, S., et al., *Massive xanthomatosis and atherosclerosis in cholesterol-fed low density lipoprotein receptor-negative mice.* J Clin Invest, 1994. **93**(5): p. 1885-93.

55. Breslow, J.L., *Mouse models of atherosclerosis.* Science, 1996. **272**(5262): p. 685-8.

56. Paigen, B., et al., *Variation in susceptibility to atherosclerosis among inbred strains of mice.* Atherosclerosis, 1985. **57**(1): p. 65-73.

57. Paigen, B., et al., *Quantitative assessment of atherosclerotic lesions in mice.* Atherosclerosis, 1987. **68**(3): p. 231-40.

58. Paigen, B., et al., *Comparison of atherosclerotic lesions and HDL-lipid levels in male, female, and testosterone-treated female mice from strains C57BL/6, BALB/c, and C3H.* Atherosclerosis, 1987. **64**(2-3): p. 215-21.

59. Reddick, R.L., S.H. Zhang, and N. Maeda, *Atherosclerosis in mice lacking apo E. Evaluation of lesional development and progression.* Arterioscler Thromb, 1994. **14**(1): p. 141-7.

60. DeStefano, F., et al., *Dental disease and risk of coronary heart disease and mortality.* BMJ, 1993. **306**(6879): p. 688-91.

61. Mattila, K.J., et al., *Dental infection and the risk of new coronary events: prospective study of patients with documented coronary artery disease.* Clin Infect Dis, 1995. **20**(3): p. 588-92.

62. Joshipura, K.J., et al., *Poor oral health and coronary heart disease.* J Dent Res, 1996. **75**(9): p. 1631-6.

63. Beck, J., et al., *Periodontal disease and cardiovascular disease.* J Periodontol, 1996. **67 Suppl**: p. 1123-37.

64. Morrison, H.I., L.F. Ellison, and G.W. Taylor, *Periodontal disease and risk of fatal coronary heart and cerebrovascular diseases.* J Cardiovasc Risk, 1999. **6**(1): p. 7-11.

65. Hujoel, P.P., et al., *Periodontal disease and coronary heart disease risk.* JAMA, 2000. **284**(11): p. 1406-10.

66. Wu, T., et al., *Periodontal disease and risk of cerebrovascular disease: the first national health and nutrition examination survey and its follow-up study.* Arch Intern Med, 2000. **160**(18): p. 2749-55.

67. Howell, T.H., et al., *Periodontal disease and risk of subsequent cardiovascular disease in U.S. male physicians.* J Am Coll Cardiol, 2001. **37**(2): p. 445-50.

68. Genco, R., S. Offenbacher, and J. Beck, *Periodontal disease and cardiovascular disease: epidemiology and possible mechanisms.* J Am Dent Assoc, 2002. **133 Suppl**: p. 14S-22S.

69. Lowe, G.D., *The relationship between infection, inflammation, and cardiovascular disease: an overview.* Ann Periodontol, 2001. **6**(1): p. 1-8.

70. Deshpande, R.G., M.B. Khan, and C.A. Genco, *Invasion of aortic and heart endothelial cells by Porphyromonas gingivalis.* Infect Immun, 1998. **66**(11): p. 5337-43.

71. Progulske-Fox, A., et al., *Porphyromonas gingivalis virulence factors and invasion of cells of the cardiovascular system.* J Periodontal Res, 1999. **34**(7): p. 393-9.

72. Varlamos, S.E., *Novel Ceramides of Porphyromonas gingivalis Recovered in Human Carotid Endarterectomy Samples*, in *Department of Periodontology*. 2003, University of Connecticut Health Center: Farmington, CT.

73. Garbus, J., et al., *The rapid incorporation of phosphate into mitochondrial lipids.* J Biol Chem, 1963. **238**: p. 69-63.

74. Bligh, E.G. and W.J. Dyer, *A rapid method of total lipid extraction and purification.* Can J Biochem Physiol, 1959. **37**: p. 911-917.

75. Richards, D. and R.B. Rutherford, *The effects of interleukin 1 on collagenolytic activity and prostaglandin-E secretion by human periodontal-ligament and gingival fibroblast.* Arch Oral Biol, 1988. **33**(4): p. 237-43.

76. Luderer, J.R., D.L. Riley, and L.M. Demers, *Rapid extraction of arachidonic acid metabolites utilizing octadecyl reversed-phase columns.* J. Chromatography, 1983. **273**: p. 402-409.

77. Waddell, K.A., et al., *Quantitative analysis of prostanoids in biological fluids by combined capillary column gas chromatography negative ion chemical ionization mass spectrometry.* Biomed Mass Spectrom, 1984. **11**(2): p. 68-74.

78. Humason, G.L., *Animal Tissue Techniques*. 2nd ed. 1967, San Francisco: W. H. Freeman.

79. Zhang, S.H., et al., *Diet-induced atherosclerosis in mice heterozygous and homozygous for apolipoprotein E gene disruption.* J Clin Invest, 1994. **94**(3): p. 937-45.

80. Saikku, P., et al., *Serological evidence of an association of a novel Chlamydia, TWAR, with chronic coronary heart disease and acute myocardial infarction.* Lancet, 1988. **2**(8618): p. 983-6.

81. Farsak, B., et al., *Detection of Chlamydia pneumoniae and Helicobacter pylori DNA in human atherosclerotic plaques by PCR.* J Clin Microbiol, 2000. **38**(12): p. 4408-11.

82. Melnick, J.L., et al., *Cytomegalovirus DNA in arterial walls of patients with atherosclerosis.* J Med Virol, 1994. **42**(2): p. 170-4.

83. Taylor-Robinson, D. and B.J. Thomas, *Chlamydia pneumoniae in atherosclerotic tissue.* J Infect Dis, 2000. **181 Suppl 3**: p. S437-40.

84. Karlsson, L., et al., *Detection of viable Chlamydia pneumoniae in abdominal aortic aneurysms.* Eur J Vasc Endovasc Surg, 2000. **19**(6): p. 630-5.

85. Fong, I.W., *Infections and their role in atherosclerotic vascular disease.* J Am Dent Assoc, 2002. **133 Suppl**: p. 7S-13S.

86. Haraszthy, V.I., et al., *Identification of periodontal pathogens in atheromatous plaques.* J Periodontol, 2000. **71**(10): p. 1554-60.

87. Dorn, B.R., W.A. Dunn, Jr., and A. Progulske-Fox, *Invasion of human coronary artery cells by periodontal pathogens.* Infect Immun, 1999. **67**(11): p. 5792-8.

88. Li, L., et al., *Porphyromonas gingivalis infection accelerates the progression of atherosclerosis in a heterozygous apolipoprotein E-deficient murine model.* Circulation, 2002. **105**(7): p. 861-7.

89. Lalla, E., et al., *Oral infection with a periodontal pathogen accelerates early atherosclerosis in apolipoprotein E-null mice.* Arterioscler Thromb Vasc Biol, 2003. **23**(8): p. 1405-11.

90. Martin, L. and A.H. Anton, *Toxicity of acids and bases after intraperitoneal injection.* Eur J Pharmacol, 1970. **11**(1): p. 38-47.

91. Livy, D.J., S.E. Parnell, and J.R. West, *Blood ethanol concentration profiles: a comparison between rats and mice.* Alcohol, 2003. **29**(3): p. 165-71.

92. Aston, R. and S. Stolman, *Influence of route and concentration of ethanol upon central depressant effect in the mouse.* Proc Soc Exp Biol Med, 1966. **123**(2): p. 496-8.

93. Stewart-Phillips, J.L. and J. Lough, *Pathology of atherosclerosis in cholesterol-fed, susceptible mice.* Atherosclerosis, 1991. **90**(2-3): p. 211-8.

94. Nishina, P.M., et al., *Effects of dietary fats from animal and plant sources on diet-induced fatty streak lesions in C57BL/6J mice.* J Lipid Res, 1993. **34**(8): p. 1413-22.

95. Beck, J.D., et al., *Periodontitis: a risk factor for coronary heart disease?* Ann Periodontol, 1998. **3**(1): p. 127-41.